

ornl

**OAK RIDGE
NATIONAL
LABORATORY**

MARTIN MARIETTA

OPERATED BY
MARTIN MARIETTA ENERGY SYSTEMS, INC.
FOR THE UNITED STATES
DEPARTMENT OF ENERGY

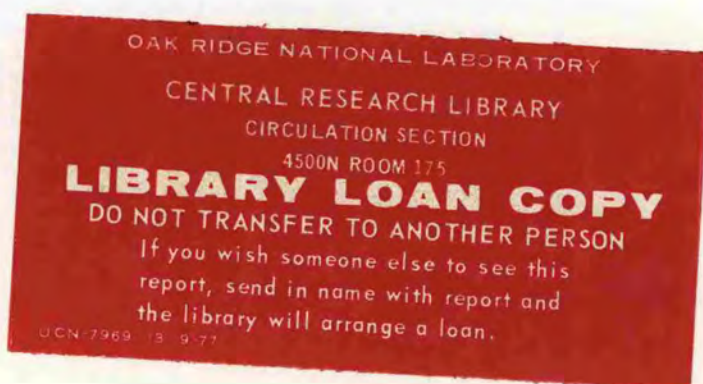


**NUREG/CR-4105
(ORNL/TM-9506)**

An Assessment of Thermal Gradient Tube Results from the HI Series of Fission Product Release Tests

K. S. Norwood

Prepared for the
U.S. Nuclear Regulatory Commission
Office of Nuclear Regulatory Research
Under Interagency Agreement DOE 40-551-75



NOTICE

Availability of Reference Materials Cited in NRC Publications

Most documents cited in NRC publications will be available from one of the following sources:

1. The NRC Public Document Room, 1717 H Street, N.W., Washington, DC 20555
2. The NRC/GPO Sales Program, U.S. Nuclear Regulatory Commission, Washington, DC 20555
3. The National Technical Information Service, Springfield, VA 22161

Although the listing that follows represents the majority of documents cited in NRC publications, it is not intended to be exhaustive.

Referenced documents available for inspection and copying for a fee from the NRC Public Document Room include NRC correspondence and internal NRC memoranda; NRC Office of Inspection and Enforcement bulletins, circulars, information notices, inspection and investigation notices; Licensee Event Reports; vendor reports and correspondence; Commission papers; and applicant and licensee documents and correspondence.

The following documents in the NUREG series are available for purchase from the NRC/GPO Sales Program: formal NRC staff and contractor reports, NRC-sponsored conference proceedings, and NRC booklets and brochures. Also available are Regulatory Guides, NRC regulations in the *Code of Federal Regulations*, and *Nuclear Regulatory Commission Issuances*.

Documents available from the National Technical Information Service include NUREG series reports and technical reports prepared by other federal agencies and reports prepared by the Atomic Energy Commission, forerunner agency to the Nuclear Regulatory Commission.

Documents available from public and special technical libraries include all open literature items, such as books, journal and periodical articles, and transactions. *Federal Register* notices, federal and state legislation, and congressional reports can usually be obtained from these libraries.

Documents such as theses, dissertations, foreign reports and translations, and non-NRC conference proceedings are available for purchase from the organization sponsoring the publication cited.

Single copies of NRC draft reports are available free, to the extent of supply, upon written request to the Division of Technical Information and Document Control, U.S. Nuclear Regulatory Commission, Washington, DC 20555.

Copies of industry codes and standards used in a substantive manner in the NRC regulatory process are maintained at the NRC Library, 7920 Norfolk Avenue, Bethesda, Maryland, and are available there for reference use by the public. Codes and standards are usually copyrighted and may be purchased from the originating organization or, if they are American National Standards, from the American National Standards Institute, 1430 Broadway, New York, NY 10018.

Notice

This report was prepared as an account of work sponsored by an agency of the United States Government. Neither the United States Government nor any agency thereof, nor any of their employees, makes any warranty, express or implied, or assumes any legal liability or responsibility for the accuracy, completeness, or usefulness of any information, apparatus, product, or process disclosed, or represents that its use would not infringe privately owned rights. Reference herein to any specific commercial product, process, or service by trade name, trademark, manufacturer, or otherwise, does not necessarily constitute or imply its endorsement, recommendation, or favoring by the United States Government or any agency thereof. The views and opinions of authors expressed herein do not necessarily state or reflect those of the United States Government or any agency thereof.

NUREG/CR-4105
ORNL/TM-9506
Dist. Category R3

Chemical Technology Division

AN ASSESSMENT OF THERMAL GRADIENT TUBE RESULTS FROM THE HI SERIES
OF FISSION PRODUCT RELEASE TESTS

K. S. Norwood*

* On temporary assignment at Oak Ridge National Laboratory from the
United Kingdom Atomic Energy Authority.

Manuscript Completed — March 1984
Date of Issue — March 1985

NOTICE This document contains information of a preliminary nature.
It is subject to revision or correction and therefore does not represent a
final report.

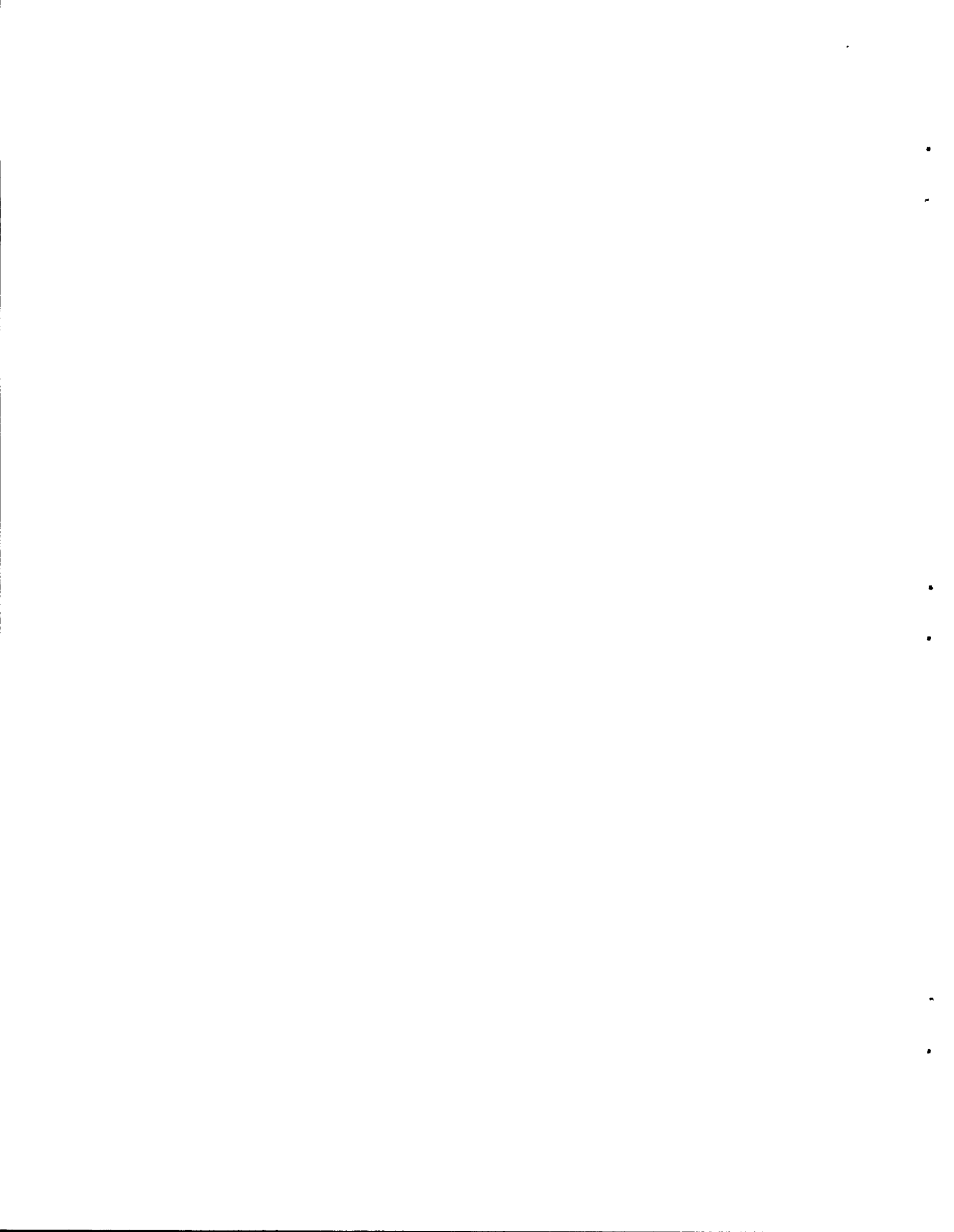
Prepared for the
U.S. Nuclear Regulatory Commission
Office of Nuclear Regulatory Research
Washington, D.C.
under Interagency Agreement DOE 40-551-75

NRC FIN No. B0127

Prepared by the
OAK RIDGE NATIONAL LABORATORY
Oak Ridge, Tennessee 37831
operated by
MARTIN MARIETTA ENERGY SYSTEMS, INC.
for the
U.S. DEPARTMENT OF ENERGY
under Contract No. DC-AC05-84OR21400



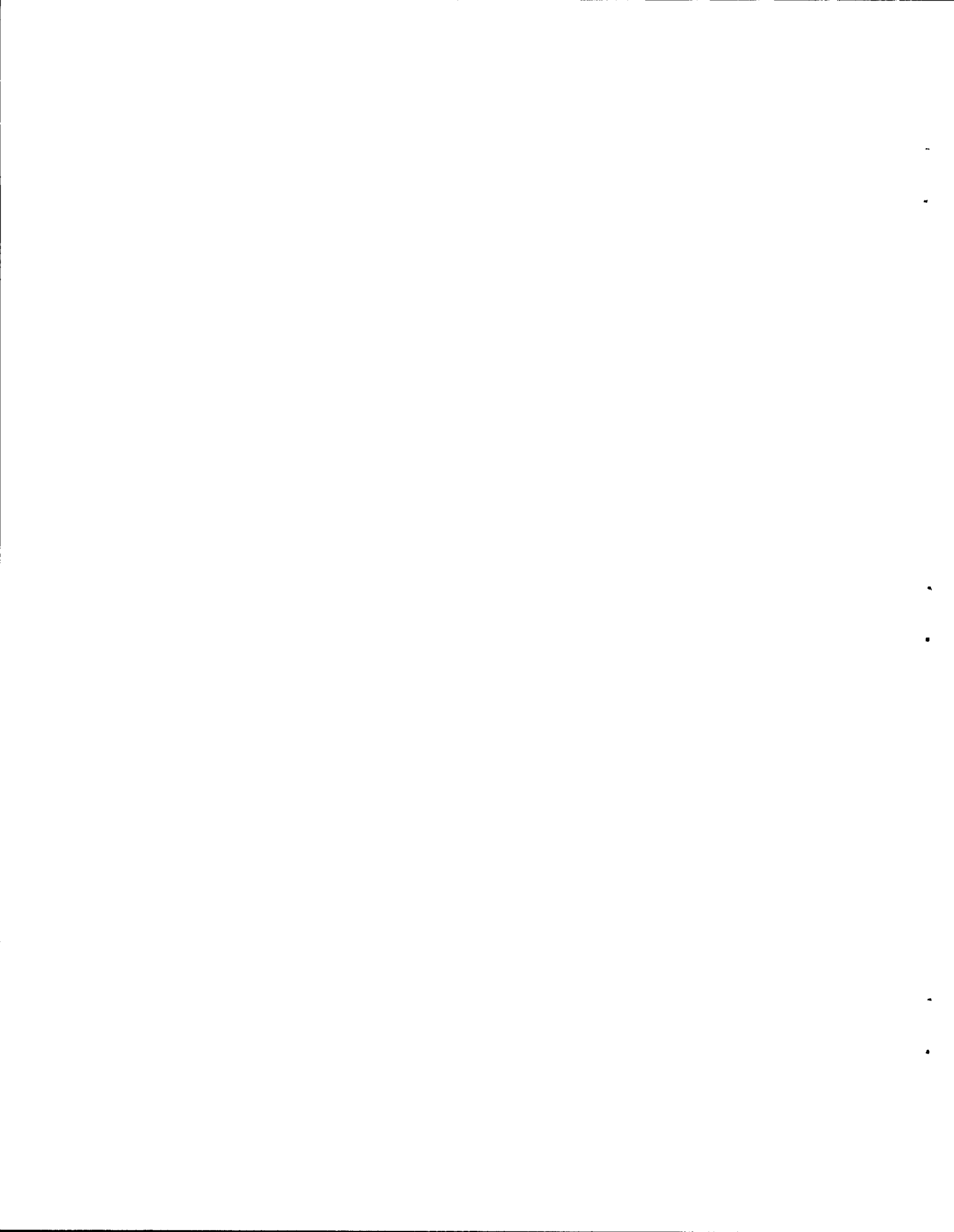
3 4456 0040402 4



ABSTRACT

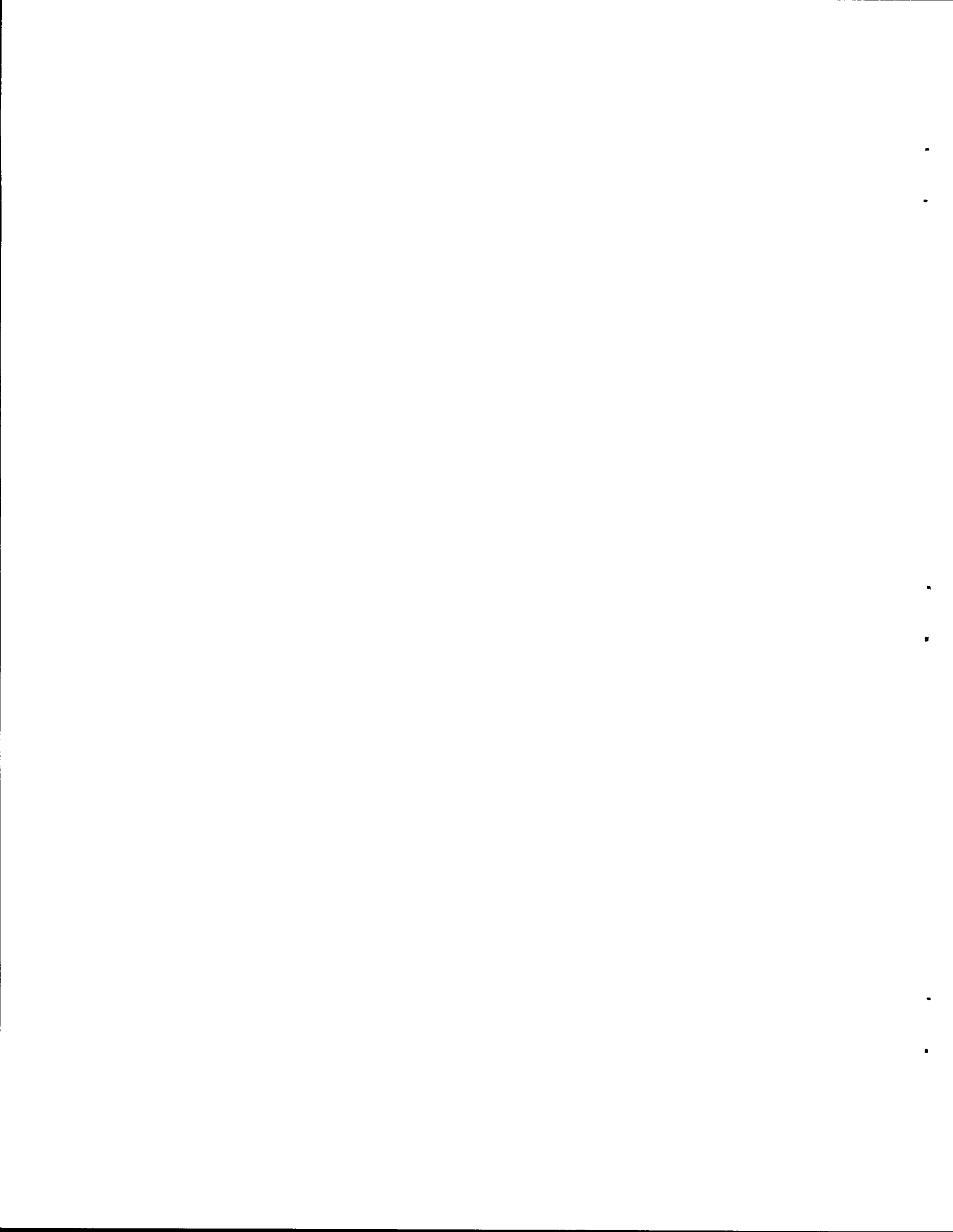
A thermal gradient tube was used to analyze fission product vapors released from fuel heated in the HI test series. Complete deposition profiles were obtained for Cs, I, Ag, and Sb. The cesium profiles were complex and probably were dominated by Cs-S-O compounds formed by release of sulfur from furnace ceramics. The iodine profiles were simple, indicating that more than 99.5% of the released iodine behaved as a single non-volatile species, probably CsI. Mass transfer coefficients for this species onto platinum were estimated to be 1.9 to 5.8 cm/s. Silver was probably released in elemental form, condensed to an aerosol, and captured by filters. Antimony was released as the element and reacted rapidly with platinum (or gold) as it deposited. Antimony profiles were calculated a priori with some success.

A method was developed for isolating tellurium from platinum and mixed fission products in a form suitable for neutron activation analysis. The platinum samples were completely dissolved in acid (HCl/HNO₃), and the tellurium was precipitated on selenium carrier by reduction. Finally, tellurium was loaded onto Dowex 1X-4 ion-exchange resin for activation and analysis. Tellurium recovery was ~88%, and the theoretical sensitivity was ~30 ng.



CONTENTS

	<u>Page</u>
ABSTRACT	iii
LIST OF FIGURES	vii
LIST OF TABLES	ix
1. EXECUTIVE SUMMARY	1
2. INTRODUCTION	2
3. CESIUM BEHAVIOR	3
4. EFFECT OF BASIC AND ACIDIC LEACHES ON DEPOSITED CESIUM	3
5. IODINE BEHAVIOR	3
6. CESIUM IODIDE MASS TRANSPORT IN THE THERMAL GRADIENT TUBE	12
7. SILVER BEHAVIOR IN THE THERMAL GRADIENT TUBE	15
8. ANTIMONY BEHAVIOR IN THE THERMAL GRADIENT TUBE	19
9. POSSIBLE TELLURIUM ANALYSES	28
10. CONCLUSIONS	28
11. ACKNOWLEDGMENTS	29
12. REFERENCES	29
APPENDIXES	33
APPENDIX A. APPLICATION OF RAOULT'S LAW TO CsI TGT PROFILE	35
APPENDIX B. CALCULATION OF DIFFUSION COEFFICIENT OF ANTIMONY IN A MIXED GAS	37
APPENDIX C. CALCULATION OF ANTIMONY DEPOSITION PROFILE IN TGT	39
APPENDIX D. ESTIMATION OF THE MINIMUM DIFFUSION COEFFICIENT FOR ANTIMONY IN PLATINUM FROM THERMAL GRADIENT TUBE DATA	43
APPENDIX E. DIFFUSION COEFFICIENT OF TELLURIUM IN PLATINUM	45
APPENDIX F. ESTIMATE OF THE ACTIVITY COEFFICIENT OF ANTIMONY IN PLATINUM	49
APPENDIX G. A METHOD FOR ANALYZING THE THERMAL GRADIENT TUBE FOR TELLURIUM	51
G.1 PREPARATION OF PLATINUM FOILS DEPOSITED WITH TELLURIUM	51
G.2 RESPONSE OF PLATINUM/TELLURIUM SAMPLES TO LEACHING	51
G.3 CONDITIONING OF SOLUTION BEFORE TELLURIUM PRECIPITATION	55
G.4 PRECIPITATION OF TELLURIUM ON SELENIUM	55
G.5 PREPARATION OF ION-EXCHANGE RESIN LOADED WITH TELLURIUM	56
G.6 APPLICATION	56
G.7 APPLICATION TO A STAINLESS STEEL THERMAL GRADIENT TUBE	57
G.8 PROCEDURE	57
G.9 ACKNOWLEDGMENTS	58



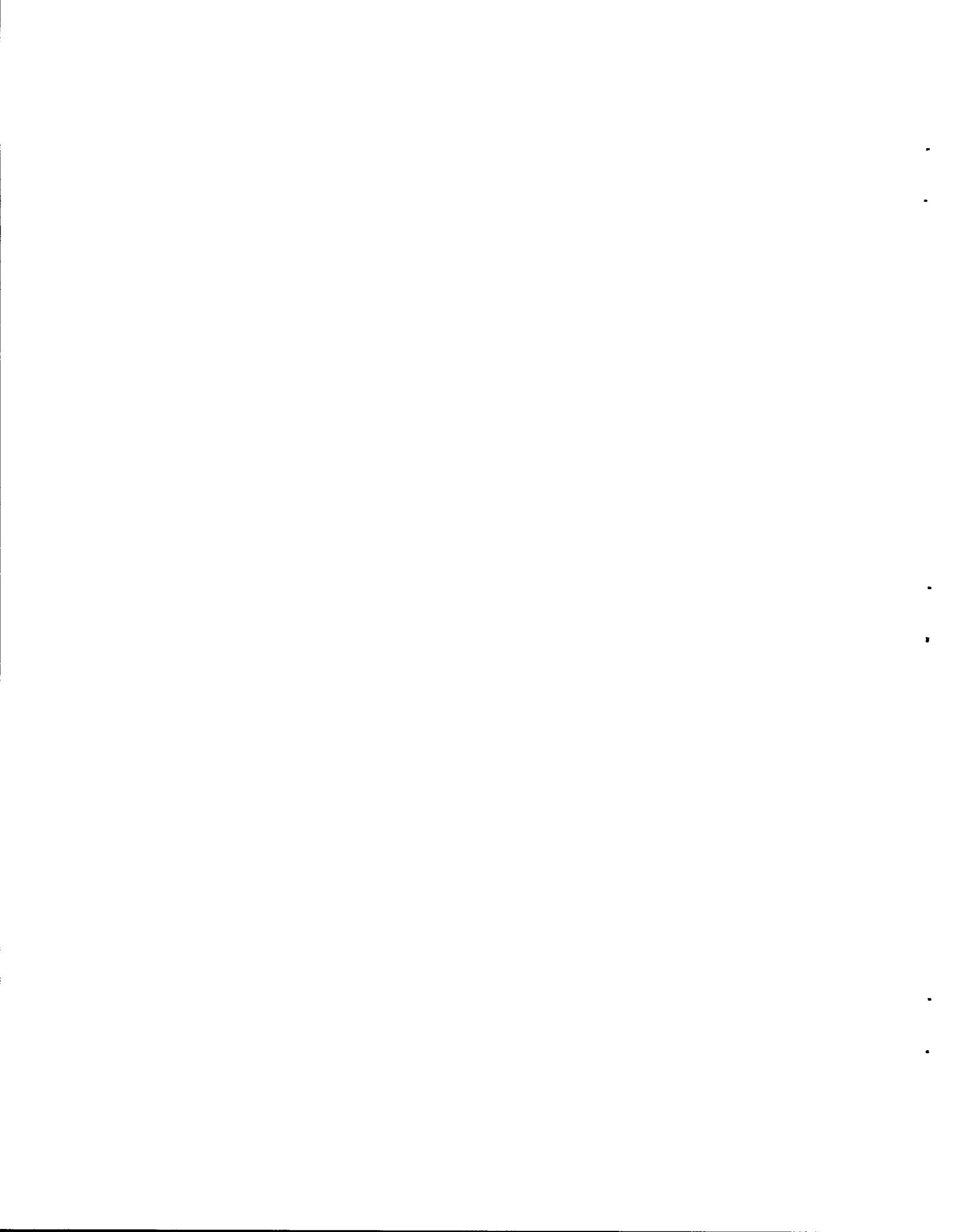
LIST OF FIGURES

<u>Figure No.</u>	<u>Page</u>
1. Surface concentration of cesium in thermal gradient tube after test HI-2	4
2. Effects of basic and acidic leaches on cesium in the thermal gradient tube after test HI-1	5
3. Effects of basic and acidic leaches on cesium in the thermal gradient tube after test HI-2	6
4. Effects of basic and acidic leaches on cesium in the thermal gradient tube after test HI-3	7
5. Effects of basic and acidic leaches on cesium in the thermal gradient tube after test HI-4	8
6. Effects of basic and acidic leaches on cesium in the thermal gradient tube after test HI-5	9
7. Surface concentration of iodine in thermal gradient tube after test HI-2	10
8. Variation of iodine peak-start temperature with CsI partial pressure in ORNL fission-product release tests	13
9. Distribution of silver in thermal gradient tube after test HI-2	16
10. Distribution of silver in thermal gradient tube after test HI-5	17
11. Surface concentration of antimony in thermal gradient tubes after fission product release experiments	20
12. Antimony deposition profiles from measured and calculated values for test HBU-11	21
13. Antimony deposition profiles from measured and calculated values for test HI-1	22
14. Antimony deposition profiles from measured and calculated values for test HI-2	23
15. Antimony deposition profiles from measured and calculated values for test HI-5	24

<u>Figure</u> <u>No.</u>	<u>Page</u>
16. Comparison of the diffusion coefficients for antimony in gold and platinum with the minimum values necessary for tests HI-1, HI-2, and HBU-11	27
C.1 Diagram of discretisation employed in antimony diffusion computer program	40
G.1 Silica apparatus for preparing platinum foils deposited with tellurium	52
G.2 Temperature history of furnace during deposition of tellurium on platinum in steam	53

LIST OF TABLES

<u>Table No.</u>		<u>Page</u>
1	Summary of basic leach data from the thermal gradient tube	10
2	Iodine behavior in the HI test series	11
3	Mass-transfer characteristics of the TGT from observed CsI deposition rates	14
G.1	Effects of leaches on tellurium deposited on platinum at 900°C	54



AN ASSESSMENT OF THERMAL GRADIENT TUBE RESULTS FROM THE HI SERIES
OF FISSION PRODUCT RELEASE TESTS

K. S. Norwood*

1. EXECUTIVE SUMMARY

The objective of this report is to summarize and interpret the results related to fission product behavior in a thermal gradient tube operated at temperatures of $\sim 850^{\circ}\text{C}$ (inlet) to $\sim 150^{\circ}\text{C}$ (outlet). The fission products were released from sections of commercial Light Water Reactor (LWR) fuel during heating at 1400 to 2000°C in an induction furnace. The released materials, which included some structural and impurity species evolved from the furnace ceramics, were carried from the furnace through the thermal gradient tube by a flowing mixture of steam and helium; depending on the temperature and extent of oxidation, varying fractions of the steam were converted to hydrogen by reaction with the Zircaloy cladding on the fuel.

The purpose of the thermal gradient tube, which was platinum of 0.36-cm diam in most tests, was to provide a relatively inert deposition surface for the gas-borne vapors; the imposed temperature gradient tended to separate the various species depending on their respective deposition temperatures. This separation of species facilitated analysis by gamma spectrometry (directly) or by neutron activation or spark-source mass spectrometry of selected samples. Complete deposition profiles were obtained for cesium, iodine, antimony, and silver, and concentrations at specific locations were obtained for a variety of other elements, including Te, Mo, Cd, Rb, Sn, Br, Mg, Ca, and S. In all tests the cesium profiles were complex and probably were dominated by Cs-S-O compounds; other analyses showed that significant masses of sulfur (apparently released from the furnace ceramics) were generally present. It should be noted, however, that this sulfur contaminant should not be present in a reactor system, where cesium behavior may be more heavily influenced by CsOH.

In contrast to the cesium profiles, the iodine profiles were invariably simple, with a single broad deposition peak. Less than 0.5% of the iodine released from the fuel was in a form (probably I_2 or CH_3I) capable of passing through both the thermal gradient tube and the following filters. The remaining $>99.5\%$ was present as an involatile species, probably CsI, of which 30 to 40% deposited in the thermal gradient tube. Based on experimental measurements, the mass transfer coefficients for this involatile species were estimated to be 1.9 to 5.8 cm/s.

Apparently, both silver and antimony were released from the fuel in elemental form. The silver appeared to condense to an aerosol, or perhaps to condense on existing aerosol particles; fairly uniform deposition of these particles occurred within the thermal gradient tube, and significant

*On temporary assignment (July 1982 to January 1984) at Oak Ridge National Laboratory from the United Kingdom Atomic Energy Authority.

fractions of the released silver passed through to the filters. Antimony, however, deposited rapidly and irreversibly on the platinum (or gold) thermal gradient tube. The principal form of the antimony vapor appeared to be Sb_2 , and a priori calculations of antimony behavior in the thermal gradient tube were reasonably successful.

Direct analysis for tellurium, another fission product of interest, was not possible. However, tellurium was separated from platinum samples during laboratory tests in a form suitable for neutron activation analysis. This technique will permit precise tellurium analysis in future fission product release tests using the platinum thermal gradient tube.

2. INTRODUCTION

The HI series of tests¹⁻⁵ is part of the U. S. Nuclear Regulatory Commission (USNRC) program to provide the basic information needed to predict the course and consequences of severe accidents in LWRs. In the test series, sections of irradiated commercial reactor fuel were heated in steam/inert gas, and the released fission products were passed through a thermal gradient tube (TGT), where they were deposited. These deposits were then measured and characterized.⁶

The thermal gradient tube was a quartz tube of 0.4-cm internal diameter, lined with platinum foil to provide an inert deposition surface. The inside surface was 0.36 cm in diameter and 30 to 36 cm long. In one experiment (C-8), the liner was a 304L stainless steel tube of 0.508-cm internal diameter. The hot gas from the furnace entered the TGT and cooled to ~ 470 K as it passed down the tube; the heat was rejected by conduction radially in the gas and then through the platinum liner, a small gas gap, and the quartz tube. The gas transit time was 40-150 ms.

A number of thermocouples on the outside of the quartz measured the temperature profile along the TGT and controlled four heaters that maintained the temperature profile. The measured temperatures fell approximately linearly from about 850°C at the gas inlet to 150°C at the gas outlet.

After the experiment, the liner was removed and its gamma spectrum determined for various locations. This defined the Cs profile. After sectioning, a basic leach removed most of the iodine and cesium, and the iodine concentrations were determined by neutron activation analysis of the leach, after treatment to remove cesium. Gamma spectrometry was again applied to the sections, and sometimes ^{110m}Ag and ^{125}Sb were then detectable.

This report should be read in conjunction with the data summary reports for each of the experiments,¹⁻⁵ which provide details of the procedures and the results. The behavior of CsI, CsOH, and Te (containing radioactive tracers) in thermal gradient tubes has been investigated and reported separately.⁷

3. CESIUM BEHAVIOR

Cesium profiles in the TGT are usually complex, as illustrated in Fig. 1. Apparently, CsOH and Cs₂O are not major constituents because they are too volatile; the major components are probably oxy-anion salts containing S (from furnace ceramics), Zr (cladding), Mo (fission product) or W (the susceptor in tests HI-1 and HI-2). These elements have been detected by spark-source mass spectrometric analysis (SSMS) in sufficient amounts to react with all the cesium in some tests. In addition, CsCO₃ may be present; carbon was released from the graphite susceptor used in tests HI-3, HI-4, and HI-5, but cannot be measured by SSMS. Cesium carbonate is moderately volatile⁸ and so is not the main cesium species on hotter areas of the TGT. Sulfur was present in all the HI series tests, but the cesium profiles in these tests were probably strongly influenced by species such as Cs₂S, Cs₂SO₃, and Cs₂SO₄ that are absent in a reactor environment.

4. EFFECT OF BASIC AND ACIDIC LEACHES ON DEPOSITED CESIUM

Figures 2 through 6 show that the basic leach dissolves cesium more readily when it is deposited at lower temperatures. On the other hand, a subsequent acidic leach dissolves all residues to the same extent.

Table 1 summarizes the basic leach data. The transition temperature (for solubility) varies from 350 to 570°C, indicating that the insoluble form is not produced by sintering, which would give a constant transition temperature. Since the transition temperature varies, the insoluble species is probably distinct and involatile, depositing on hotter portions of the TGT. The variation in transition temperature reflects a change in the gas-phase concentration of the species.

The identity of the deposited cesium species is uncertain. In an effort to correlate the behavior of this insoluble species with other elements in the TGT, the SSMS data from tests HI-1 through HI-5 were examined. Several fission product, structural, and impurity elements were present in concentrations comparable to that of cesium. Among those which appear to be possible candidates for reacting with cesium to form insoluble compounds are Mo, W, Fe, and S. The concentration of none of these, however, correlates consistently with that of the insoluble cesium species. Thus, the deposition may be the result of more than one reaction between cesium and other available elements. However, the insoluble cesium form constituted only a small fraction of the total cesium; consequently, it is unlikely to exert a significant effect on overall cesium behavior.

5. IODINE BEHAVIOR

Iodine profiles have a simple shape, as illustrated in Fig. 7. Table 2 presents data on the iodine behavior in the HI test series. Iodine that passed through the filters was in a penetrating form, either I₂ or CH₃I. In all HI tests, <0.5% of the total amount of iodine released from the fuel was in penetrating form.

ORNL DWG 82-1486

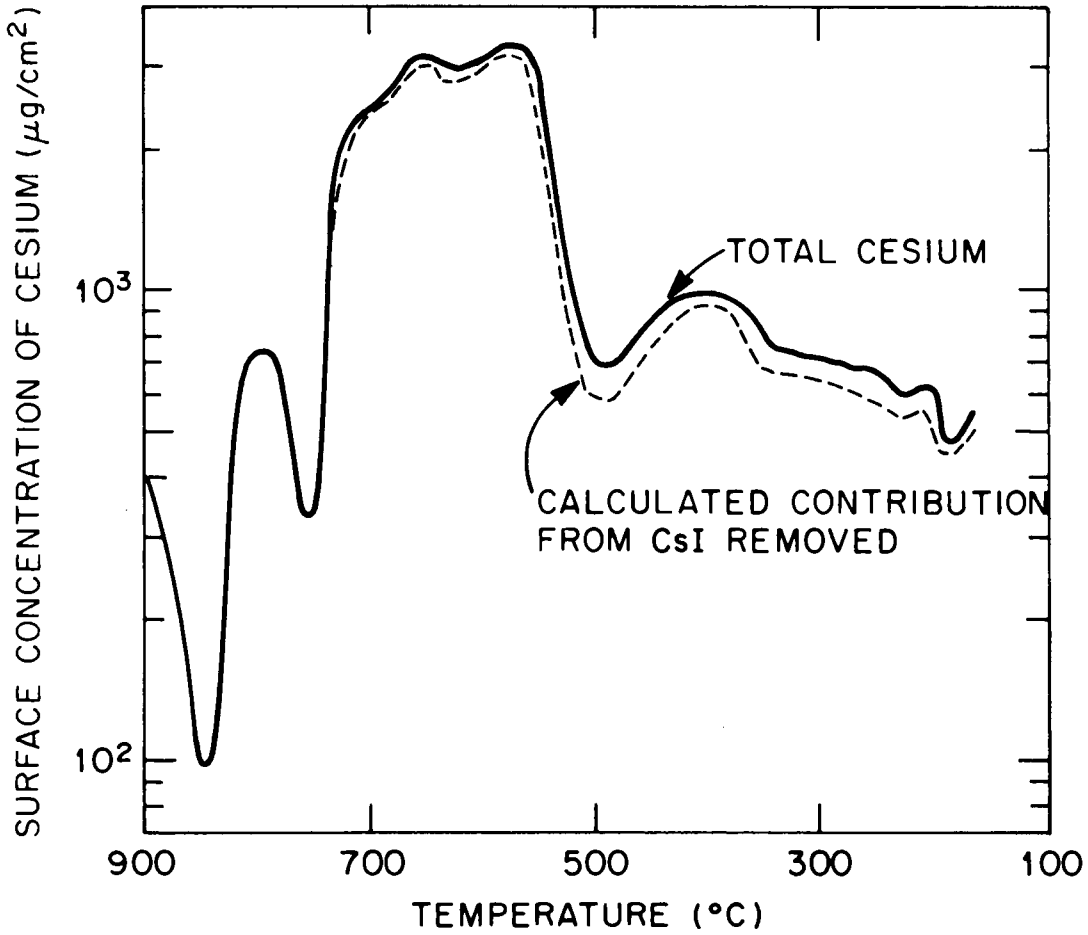


Fig. 1. Surface concentration of cesium in thermal gradient tube after test HI-2.

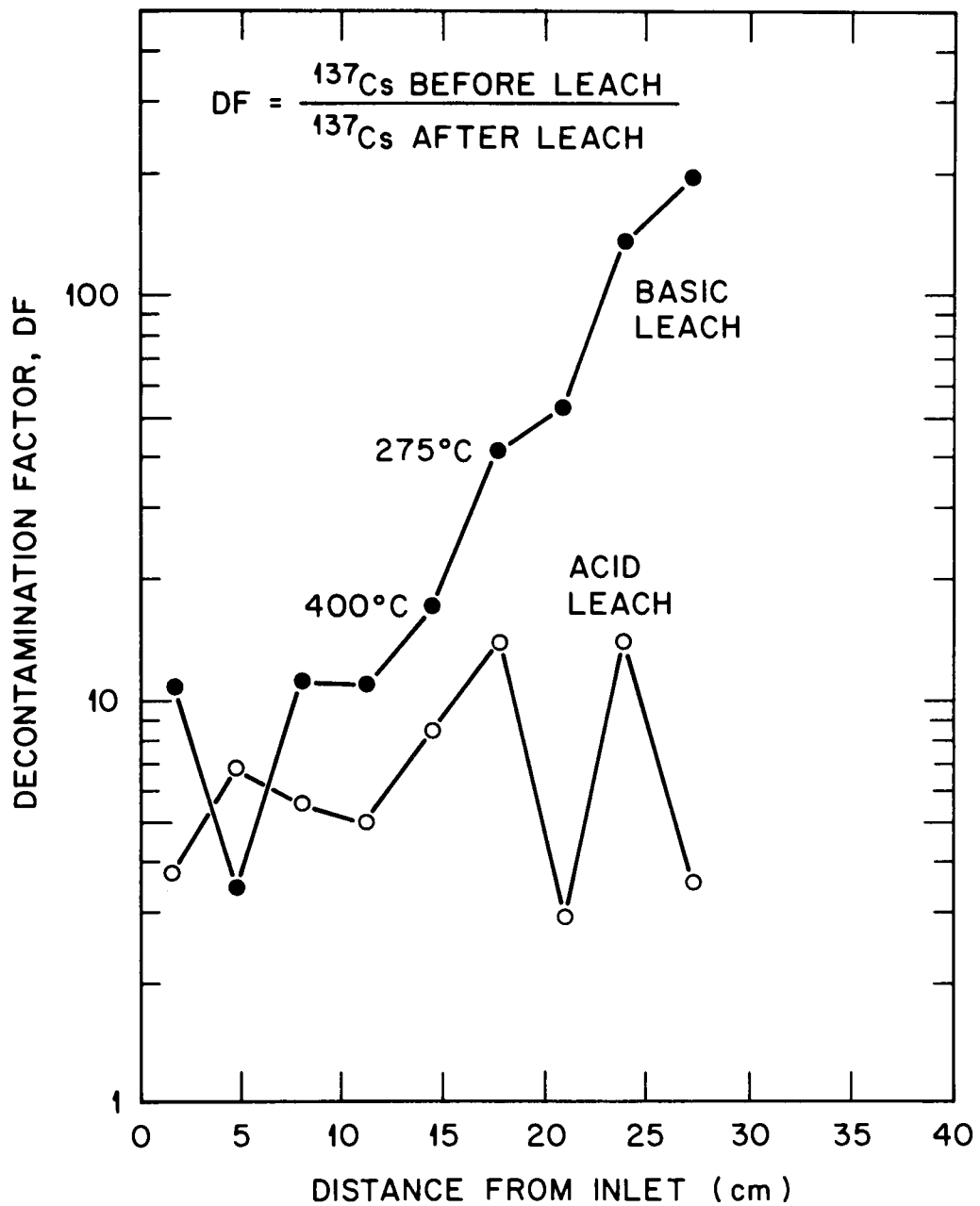


Fig. 2. Effects of basic and acidic leaches on cesium in the thermal gradient tube after test HI-1.

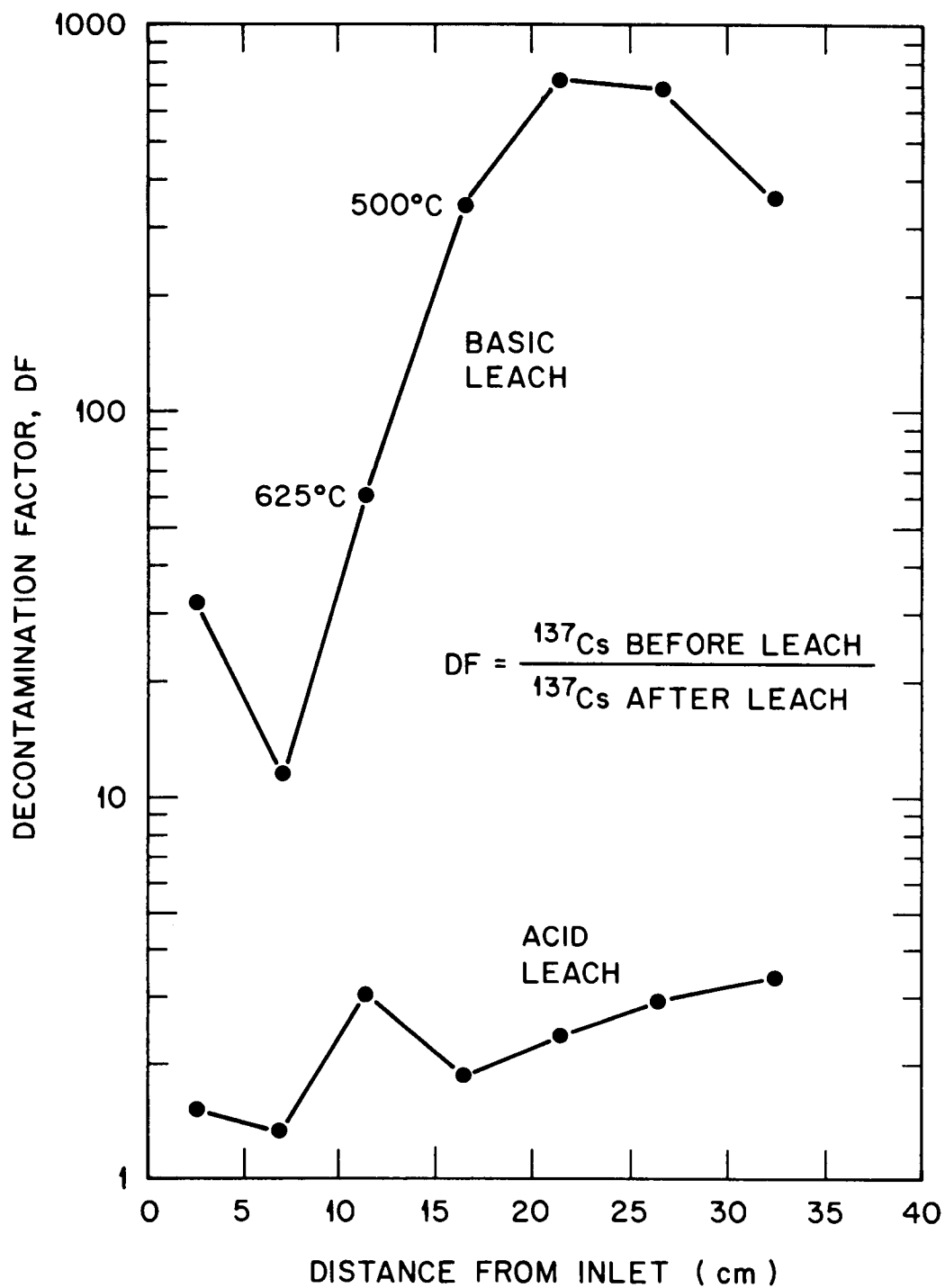


Fig. 3. Effects of basic and acidic leaches on cesium in the thermal gradient tube after test HI-2.

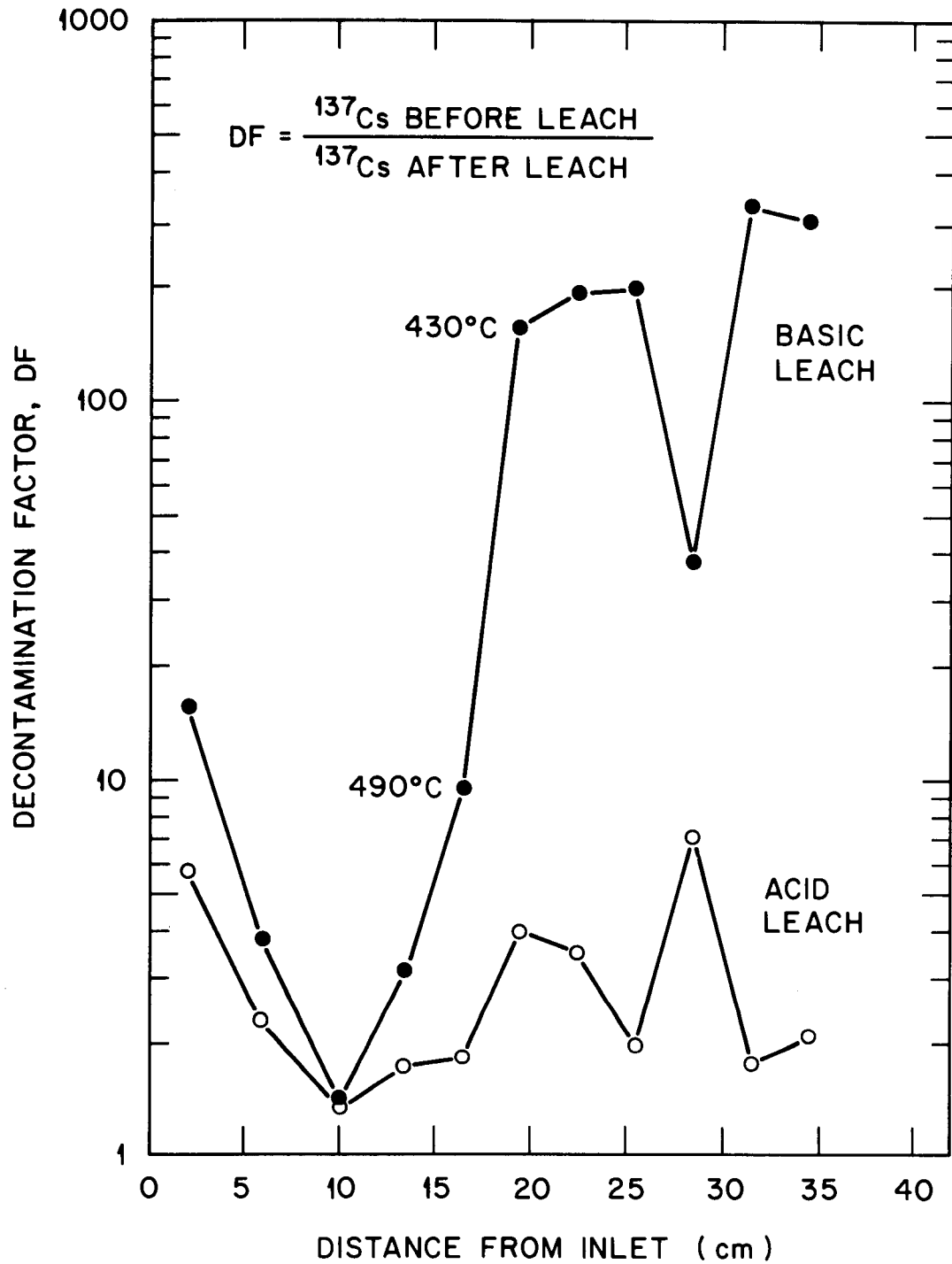


Fig. 4. Effects of basic and acidic leaches on cesium in the thermal gradient tube after test HI-3.

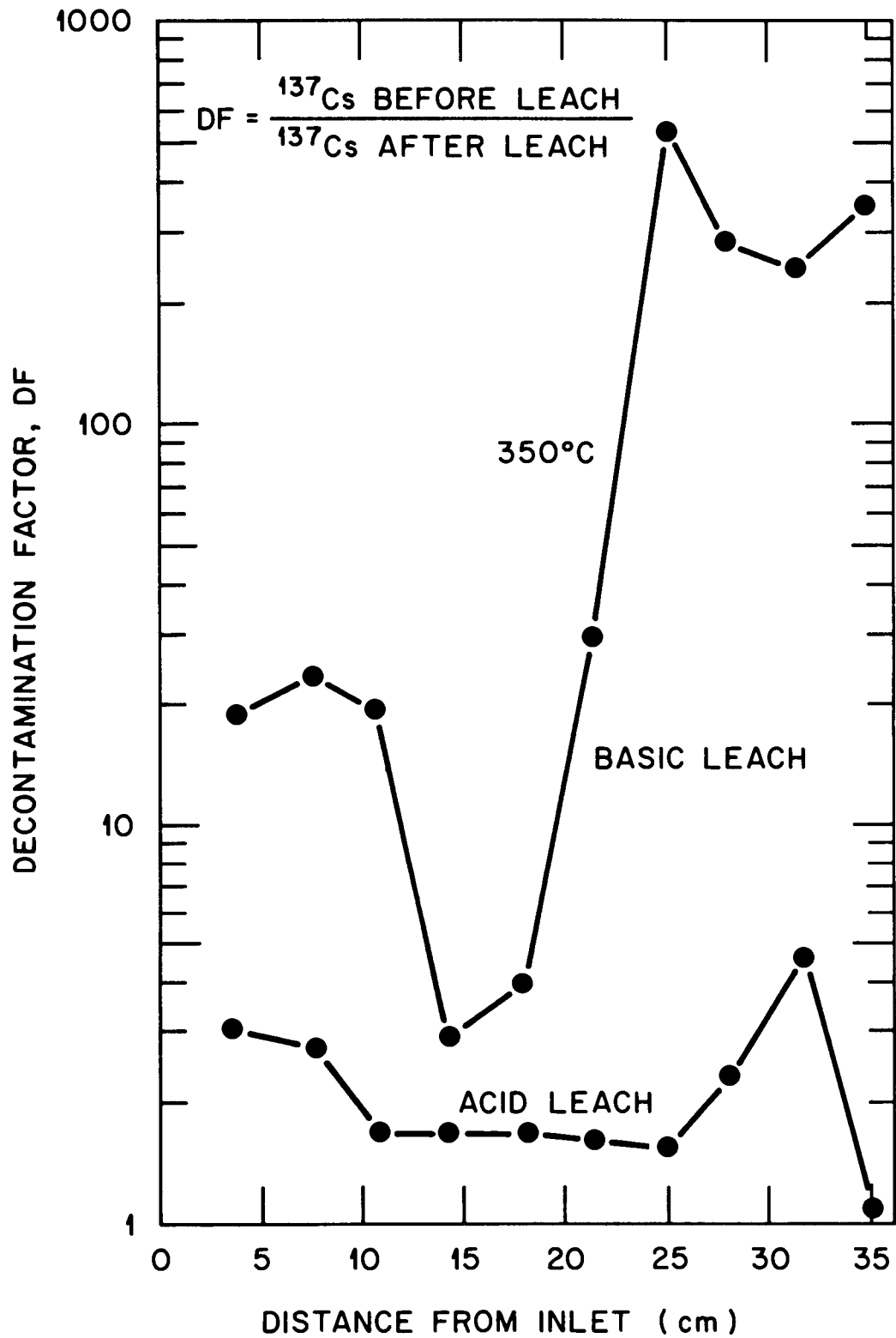


Fig. 5. Effects of basic and acidic leaches on cesium in the thermal gradient tube after test HI-4.

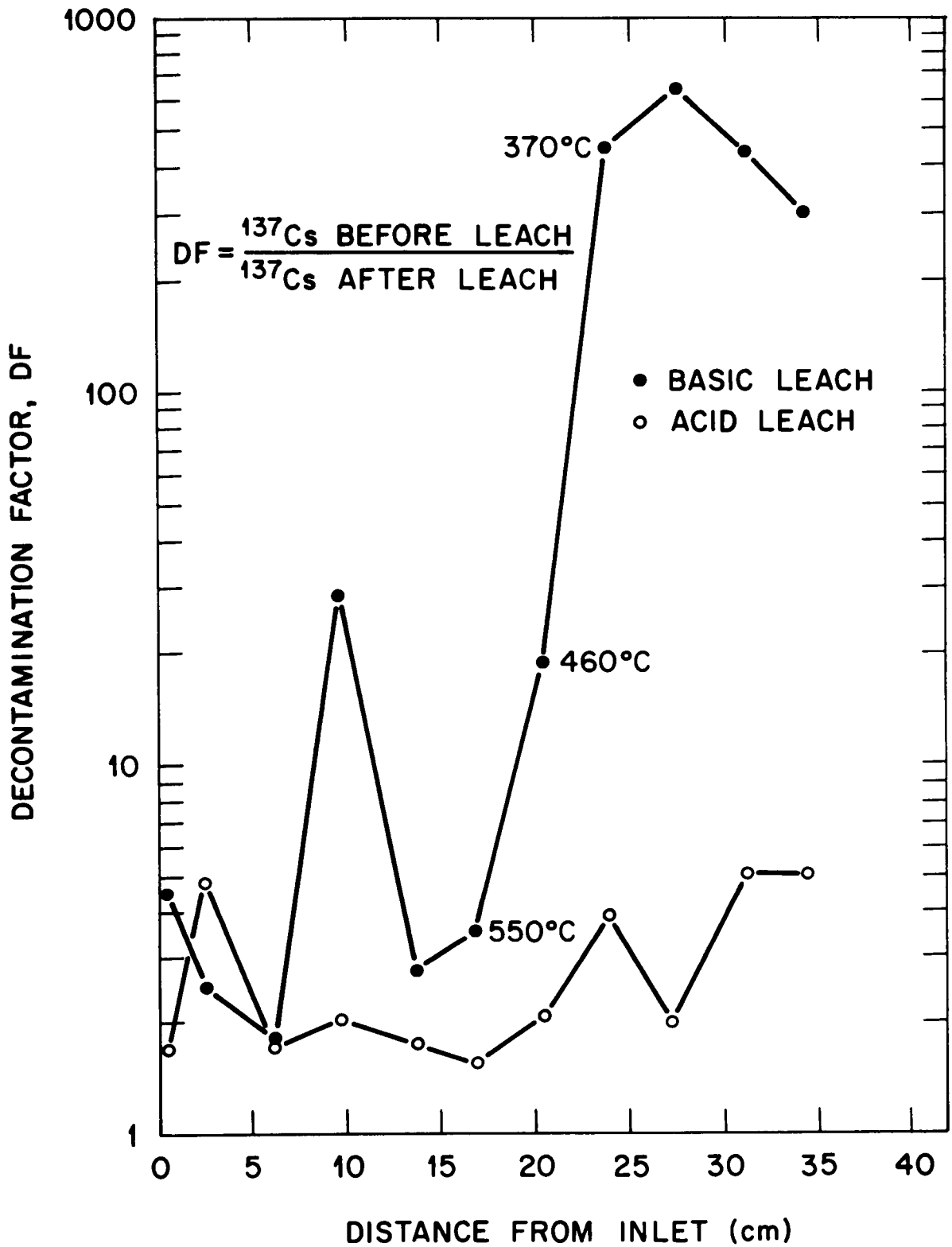


Fig. 6. Effects of basic and acidic leaches on cesium in the thermal gradient tube after test HI-5.

Table 1. Summary of basic leach data from the thermal gradient tube

Test No.	Insoluble Cs species below transition temperature (%)	Transition temperature (°C)	Insoluble Cs species above transition temperature (%)
HI-1	0.5-2.5	350	6-30
HI-2	0.14-0.3	570	1.7-9
HI-3	0.3-2.8	500	7-70
HI-4	0.2-0.4	350	3.5-34.5
HI-5	0.2-0.4	460	21-56

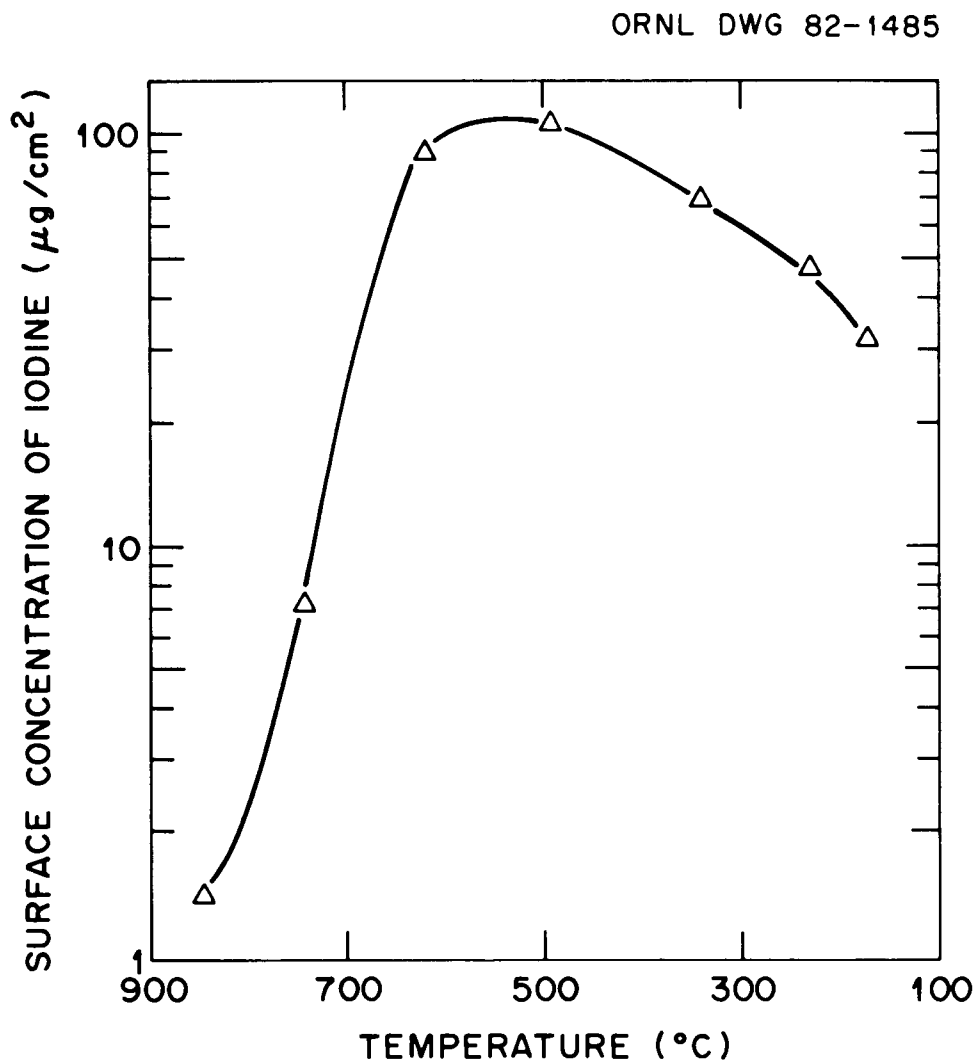


Fig. 7. Surface concentration of iodine in thermal gradient tube after test HI-2.

Table 2. Iodine behavior in the HI test series

Test No.	Maximum fuel temperature (°C)	Time (min)	Gas flow rate (mol·min ⁻¹)	Percentage inventory released ^a			Iodine peak temperature (°C)	Percentage iodine escaping TGT ^b	Percentage iodine in penetrating form ^b
				Kr	I	Cs			
HI-1	1400	30	0.06	2.83	2.04	1.75	400	59	0.49
HI-2	1700	20	0.06	51.5	53.0	50.5	600	68	0.36
HI-3	2000	20	0.03	59.0	35.4	57.7	570	65	0.003
HI-4	1850	20	0.03	21.1	24.7	31.7	510	63	0.03
HI-5	1700	20	0.02	19.8 ^c	22.9	20.8	470	67	0.07

^aBased on total inventory in the fuel specimen.

^bPercentage of total iodine released from fuel.

^cIncludes 4.0% released from fuel during irradiation.

Of the iodine species that entered the thermal gradient tube, 60–70% escaped and were intercepted by the glass wool filter downstream. The fraction does not correlate with the position of the iodine peak in the TGT, nor with the maximum fuel temperature during the test, nor with the linear gas velocity in the TGT. The 60–70% was probably an aerosol of CsI co-condensed with other cesium compounds as the gas cooled in its travel down the TGT.

This explanation is consistent with the shape of the iodine profiles. The surface concentration of iodine downstream from the peak decreased by a factor of 5 to 20, while the gas-phase concentration decreased by only 30 to 40%. Based on an assortment of data, it has been assumed that the dominant form of iodine is CsI. Therefore, some process must be transforming molecular CsI into another form in the gas phase; this process is probably aerosol condensation.

In theory, it is possible to predict the position of the upstream edge of an iodine profile from the partial pressure of iodine species in the gas, using the vapor pressure-temperature relationship for that species. Such a correlation has been demonstrated for CsI in a TGT. The upstream edge is the critical point, because there the saturated vapor pressure of the condensed iodine compound is just exceeded by the partial pressure of the species in the gas. This peak-start temperature is difficult to determine precisely. The partial pressure of iodine species averaged over the release period was calculated from the total release of iodine by dividing by the quantity of carrier gas that passed during that time. The released species was assumed to have one atom of iodine per molecule. Figure 8 plots the peak-start temperatures against partial pressure and compares them with the experimentally determined vapor pressure of CsI (using the difference between the two sets of data points as a measure of the experimental error).^{10,11} These experimentally determined vapor pressures agree well with the empirical correlations of Barin and Knacke¹² and are larger (by an average factor of ten) than the correlation of Lange.¹³

Only two experimental points lie above the band of theoretical data (Deitz¹¹ and Scheer and Fine¹⁰), and these were both from burst-release tests where the concentration of iodine species in the gas was rapidly changing and very difficult to estimate. All other points lie in or below the band, indicating that the volatility of the species is the same as or less than that of CsI. The probable explanation is that the insoluble species is CsI that deposits partially as a solid solution in another cesium compound. Raoult's Law shows that this phenomenon can reduce the vapor pressure of CsI so that it will deposit at temperatures much higher than its normal deposition temperature range (see Appendix A).

6. CESIUM IODIDE MASS TRANSPORT IN THE THERMAL GRADIENT TUBE

Table 3 lists some salient features relating to CsI deposition in the TGT for each of the five tests using a platinum-lined tube as well as for test C-8, which used a stainless steel TGT tube. The temperatures at

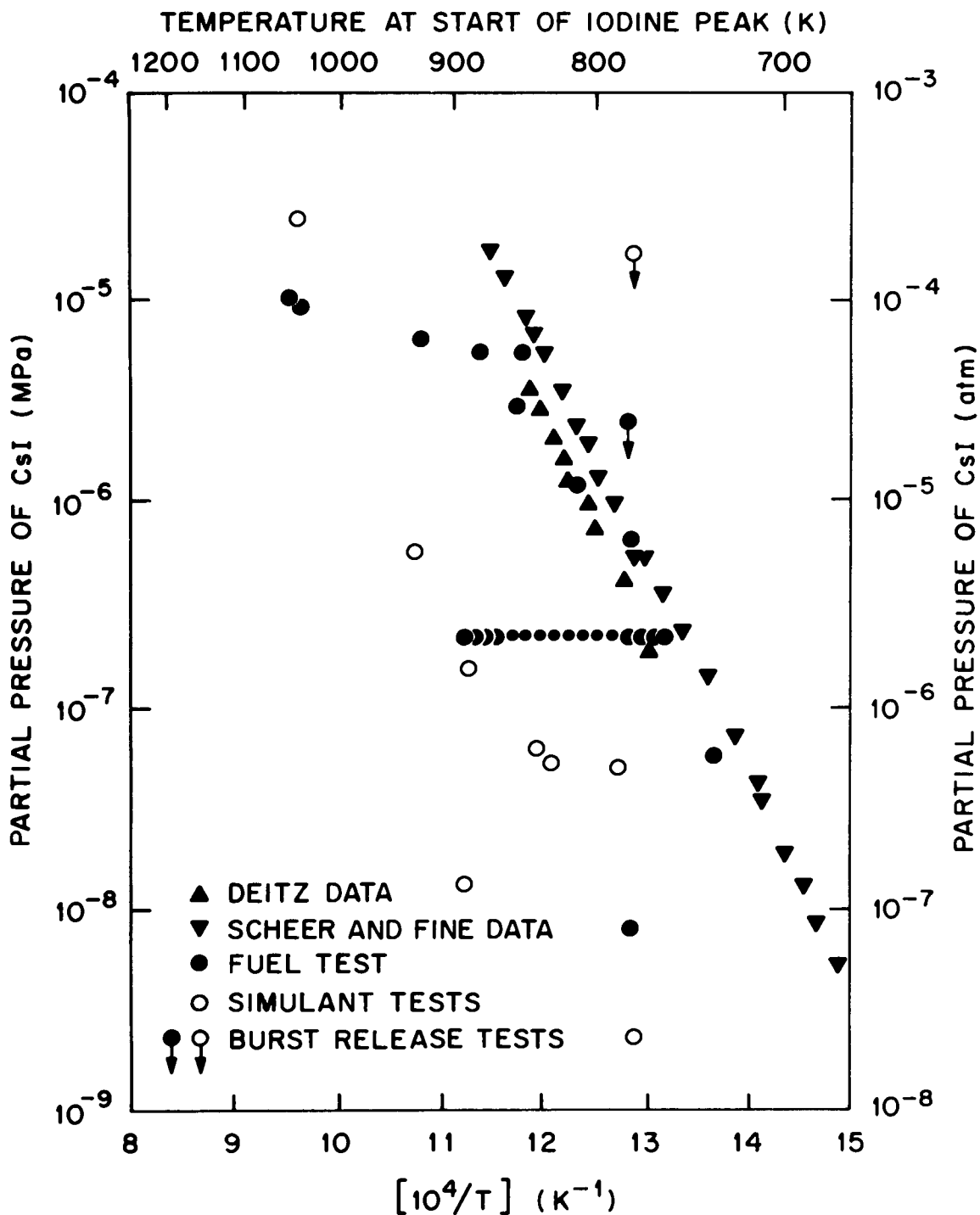


Fig. 8. Variation of iodine peak-start temperature with CsI partial pressure in ORNL fission-product release tests.

Table 3. Mass transfer characteristics of the TGT from observed CsI deposition rates

Experiment No.	TGT surface	T ^a (°C)	m ^b (μg/cm ² ·s)	C ^c (μg/cm ³)	C* ^d (μg/cm ³)	C - C*	Mass transfer coefficients (cm/s)	
							Observed ^e	Theoretical ^f
HI-1	Pt	400 ± 50	0.019	0.01	2.2 × 10 ⁻⁴	0.01	1.9	3.9
HI-2	Pt	600 ± 50	0.17	0.34	0.40			8.8
HI-3	Pt	570 ± 40	0.53	0.38	0.19	0.18	2.9	14.3
HI-4	Pt	510	0.86	0.22	0.023	0.19	4.5	20.4
HI-5	Pt	470 ± 45	0.51	0.27	0.01	0.26	2.0	15.9
C-8	SS	480	5.7	1.0	0.011	0.99	5.8	4.8

^aIodine profile peak temperature position.

^bEstimated deposition rate during run based on final value.

^cEstimated average vapor concentration based on fuel inventory and measured release.

^dEquilibrium vapor density above condensed CsI at given temperature; estimated using the vapor pressure correlation from Barin and Knacke (Ref. 12) and the mean estimated temperature.

^eCalculated from observed deposition rates.

^fEstimated from diffusion coefficients and tube dimensions.

the location of peak concentration are noted, as well as the mean deposition rates ($\mu\text{g}/\text{cm}^2\cdot\text{s}$) and gas concentrations ($\mu\text{g}/\text{cm}^3$). These latter two sets of values were estimated assuming constant rates over the test duration. The column designated C^* lists the equilibrium vapor concentrations above condensed CsI at the respective peak temperatures, calculated using the vapor pressure correlation of Barin and Knacke.¹²

The mass transfer coefficients estimated from the observed deposition rate, given in the column labeled "observed" in Table 3, were calculated using

$$m = h_m (C - C^*) ,$$

where the terms are as defined in Table 3. Uncertainties in the values for the peak temperatures, as well as in the average estimates for m and C , result in an unknown (but at least a factor of 2) degree of error in the estimated mass transfer coefficients. However, all six tests appear to have been characterized by mass transfer coefficients between 1.9 and 5.8 cm/s , based on calculations from the observed deposition rates.

The last two columns in Table 3 indicate a fair agreement between the "observed" mass transfer coefficients and the "theoretical" values estimated using the correlation for fully-developed laminar flow:

$$\text{Nu} = 4, \text{ or equivalently}$$

$$h_m = \frac{4D}{d} ,$$

where

Nu = Nusselt modulus,
 D = diffusion coefficient, cm^2/s ,
 d = TGT diameter.

The means for estimating the diffusion coefficient of Sb_2 in a mixture of $\text{H}_2\text{O}(\text{g})$, H_2 , He, and Ar is given in Appendix B. A similar procedure was used for CsI. Uncertainties in the gas composition, as well as the effects of using a time-averaged gas composition for estimation of D, contribute to an unestimated degree of uncertainty in the "theoretical" mass transfer coefficients listed in Table 3.

7. SILVER BEHAVIOR IN THE THERMAL GRADIENT TUBE

Silver has been detected in the TGT in two of the HI tests: HI-2 and HI-5. Figures 9 and 10 show the distribution profiles. In both tests, silver deposited uniformly along the length of the TGT.

Silver is difficult to detect. Spark-source mass spectrometry provides one detection method, but the results have a probable factor of 2 error, and the sampling method may be unrepresentative. Gamma spectrometry provides representative results but is difficult to apply, because

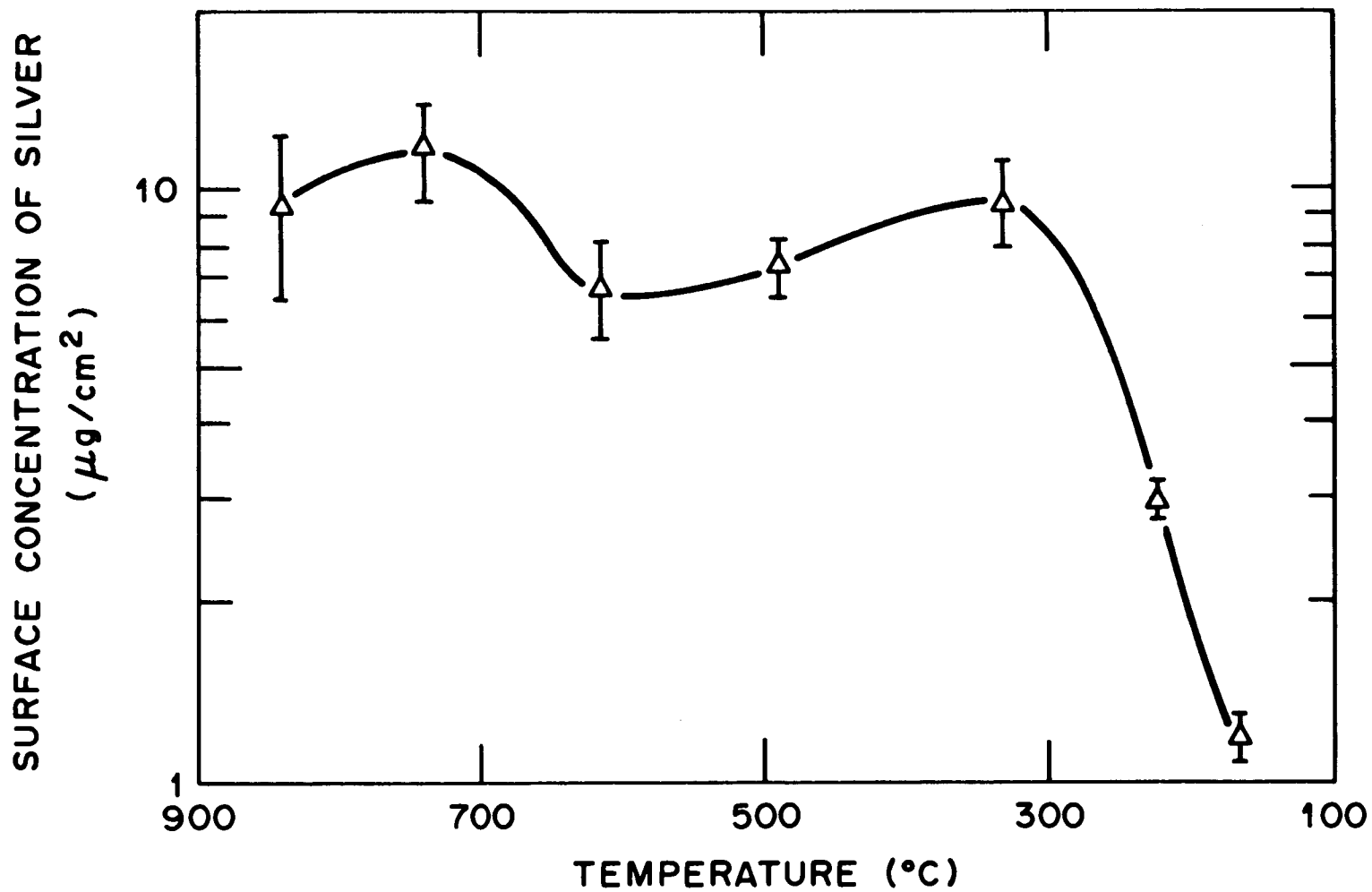


Fig. 9. Distribution of silver in thermal gradient tube after test HI-2.

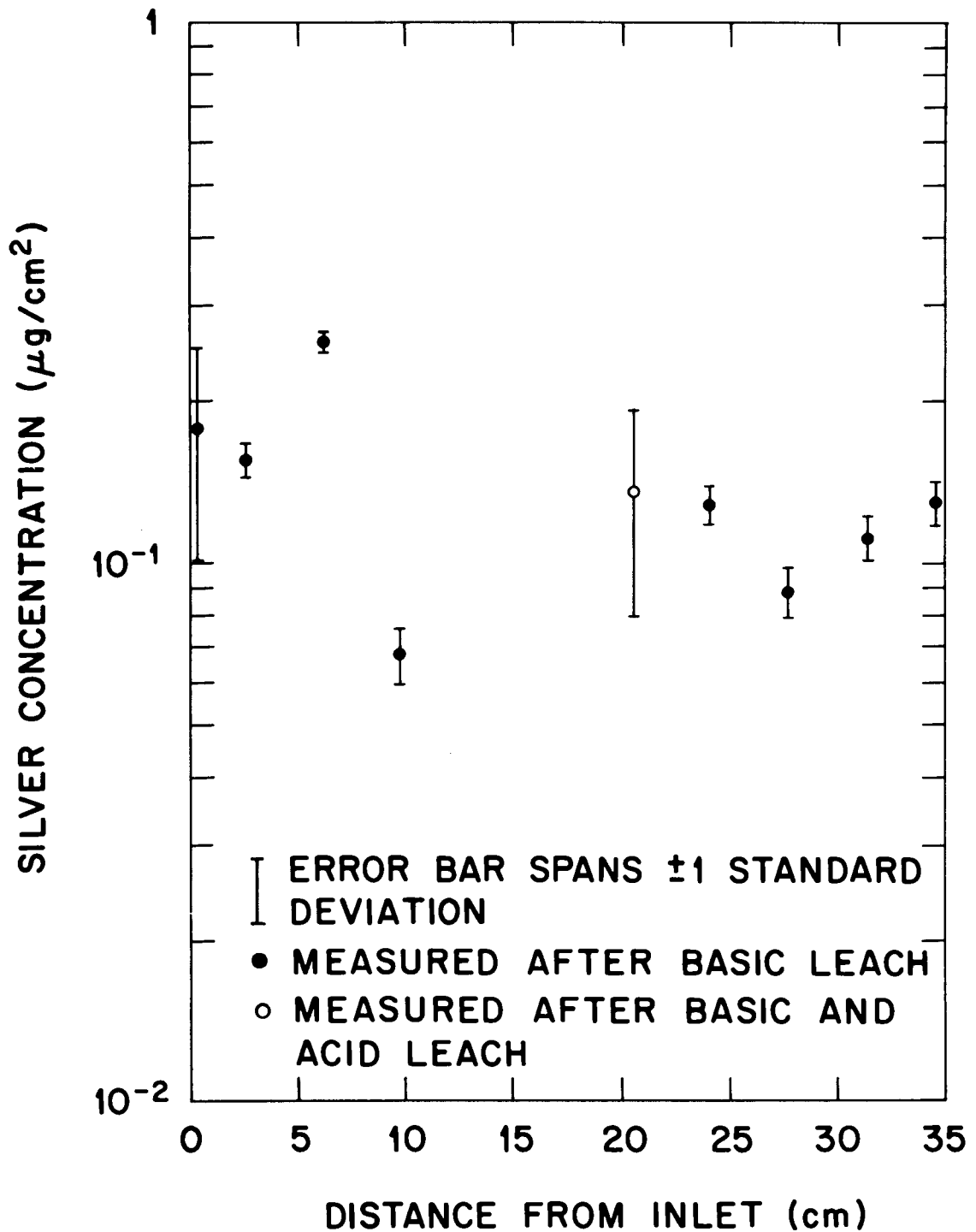


Fig. 10. Distribution of silver in thermal gradient tube after test HI-5.

^{110m}Ag has a short half-life, and test samples are usually highly active with ^{134}Cs and ^{137}Cs .

Sections of the thermal gradient tube must be leached with a basic leach ($\text{NH}_3/\text{H}_2\text{O}_2$ solution) and an acidic leach (HNO_3/HF solution) to remove cesium, before the silver can be detected by gamma spectrometry. The basic leach does not remove silver from the high-temperature end of the TGT, but the acidic leach removes small amounts of silver from the high-temperature end and much more from the low-temperature end of the tube. The flat profile shown in Fig. 10, taken after a basic leach only, represents the deposited silver. The profile shown in Fig. 9 was taken after both basic and acidic leaches, showing that silver has been lost from the low-temperature end of the TGT. In this case also, the silver deposition probably was uniform throughout the TGT.

The amounts of silver detected in tests HI-2 and HI-5 were:

Test	On TGT by gamma counting	Downstream of TGT	
		By gamma counting	By SSMS
HI-2	225 μg	23 μg	4800 μg
HI-5	3.4 μg	15 μg	Not detected

Silver deposited downstream of the TGT in test HI-2 was gamma counted after both basic and acidic leaches, so the true quantity is $>23 \mu\text{g}$ but probably $<4800 \mu\text{g}$. In test HI-5, this count was made after only the basic leach, so 15 μg is probably the true value (15 μg is probably below the SSMS detection limit, in this case). It seems probable that more silver escapes from the TGT than deposits in it.

The silver deposition behavior is that typical of aerosol particles, which have low gas-phase diffusivities. The silver species deposits slowly on the TGT surfaces and is not much depleted in the flowing gas; this causes the flat deposition profile and the large amount collected downstream on the filters.

Silver probably escapes from fuel in elemental form and would be partially soluble in nitric acid, as observed in the HI series of tests. At the hot end of the TGT, silver may partially alloy with platinum and become resistant to nitric acid. The average partial pressure of silver in tests HI-2 and HI-5 was calculated from the mass of silver released and the amount of gas flowing to be:

HI-2	4 Pa, condenses below 1090°C,
HI-5	2.4×10^{-2} Pa, condenses below 850°C.

The condensation temperatures were estimated from vapor pressure/temperature data of Hultgren et al.¹⁴ In both tests, it is possible either that elemental silver condenses alone or that it condenses on a preexisting aerosol before entering the TGT or very soon thereafter.

In conclusion, the silver behavior found in the HI series of tests is consistent with its release from the fuel in elemental form.

8. ANTIMONY BEHAVIOR IN THE THERMAL GRADIENT TUBE

Antimony has been detected as ^{125}Sb in the TGTs from four experiments: HBU-11 (Ref. 15), HI-1 (Ref. 1), HI-2 (Ref. 2), and HI-5 (Ref. 5). Figure 11 shows the deposition profiles from HBU-11, HI-1, and HI-2.

The surface concentration of antimony declines exponentially along the tube, and the partial pressure of antimony in the gas also decreases, although by a smaller factor. This behavior is typical of a species that condenses or reacts irreversibly with platinum at all temperatures attained in the TGT. For such a species,

$$R = k D C_g ,$$

where

R = rate of deposition on surface (α surface concentration of antimony) ($\text{molecules}\cdot\text{cm}^{-2}\cdot\text{s}^{-1}$),

k = proportionality constant (cm^{-1}),

D = diffusion coefficient for antimony in the gas atmosphere ($\text{cm}^2\cdot\text{s}^{-1}$),

C_g = gas-phase concentration of antimony ($\text{molecules}\cdot\text{cm}^{-3}$).

For the four experiments, the measured decreases in R and C_g along the TGT and the concomitant decreases in D are:

<u>Test No.</u>	<u>Inlet/outlet ratios</u>		
	<u>R</u>	<u>C_g</u>	<u>D</u>
HBU-11	105	45	2.3
HI-1	212	Unknown	
HI-2	1000	170	5.9
HI-5	26		

Gas-phase diffusion coefficients increase with temperature, and this may account for the residual variation in D.

The diffusion coefficient, D, can be estimated a priori from the average composition of the flowing gas and the critical constants of the various species (see Appendix B). The average concentration of antimony entering the thermal gradient tube is known, as is the gas flow rate and temperature profile. A simple calculation based on these data (see Appendix C) produces a predicted antimony profile that is illustrated, along with the measured profiles, in Figs. 12-15. This method of calculation can also be used to predict the quantity of antimony that leaves the TGT in the gas stream.

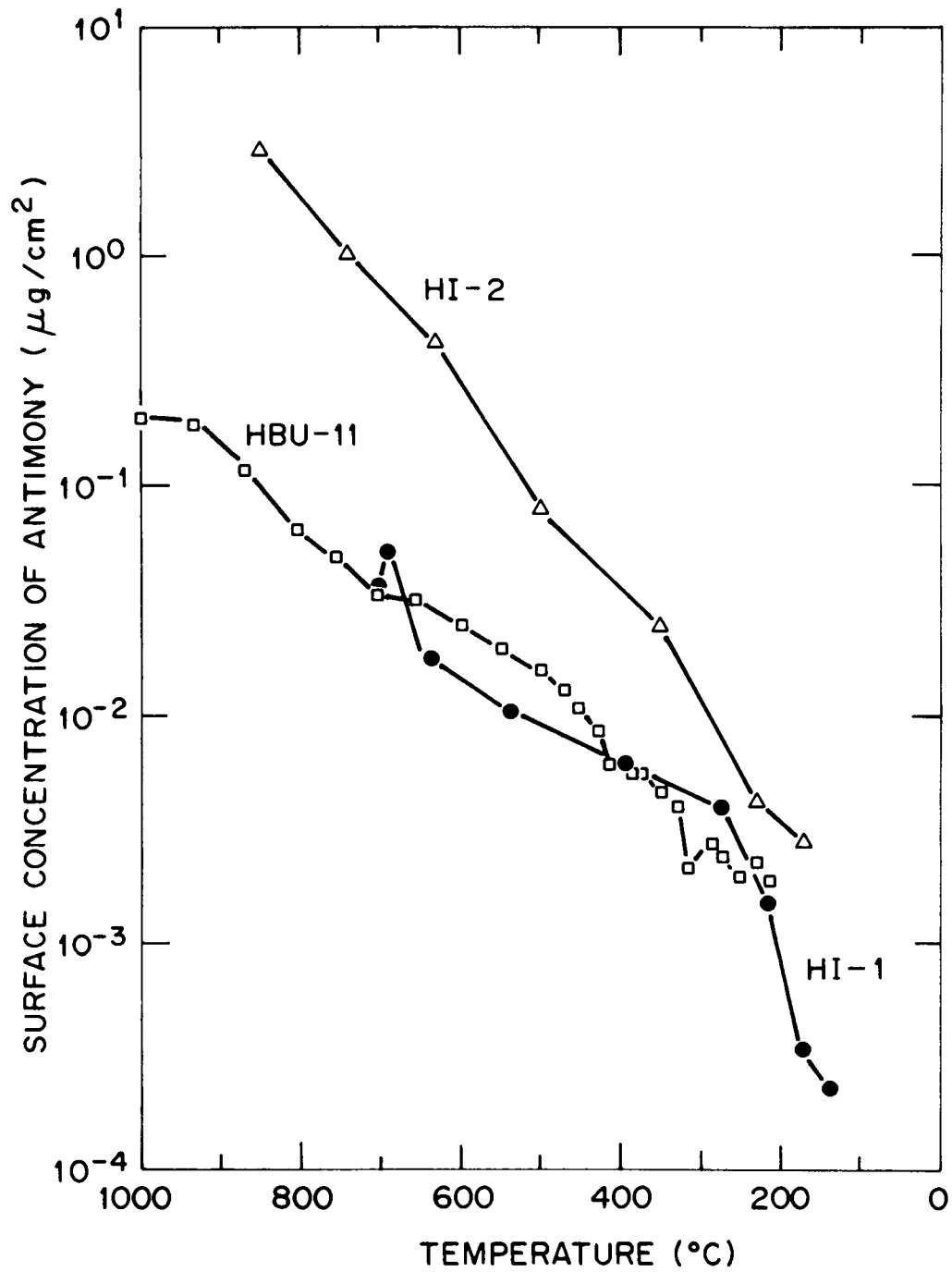


Fig. 11. Surface concentration of antimony in thermal gradient tubes after fission product release experiments.

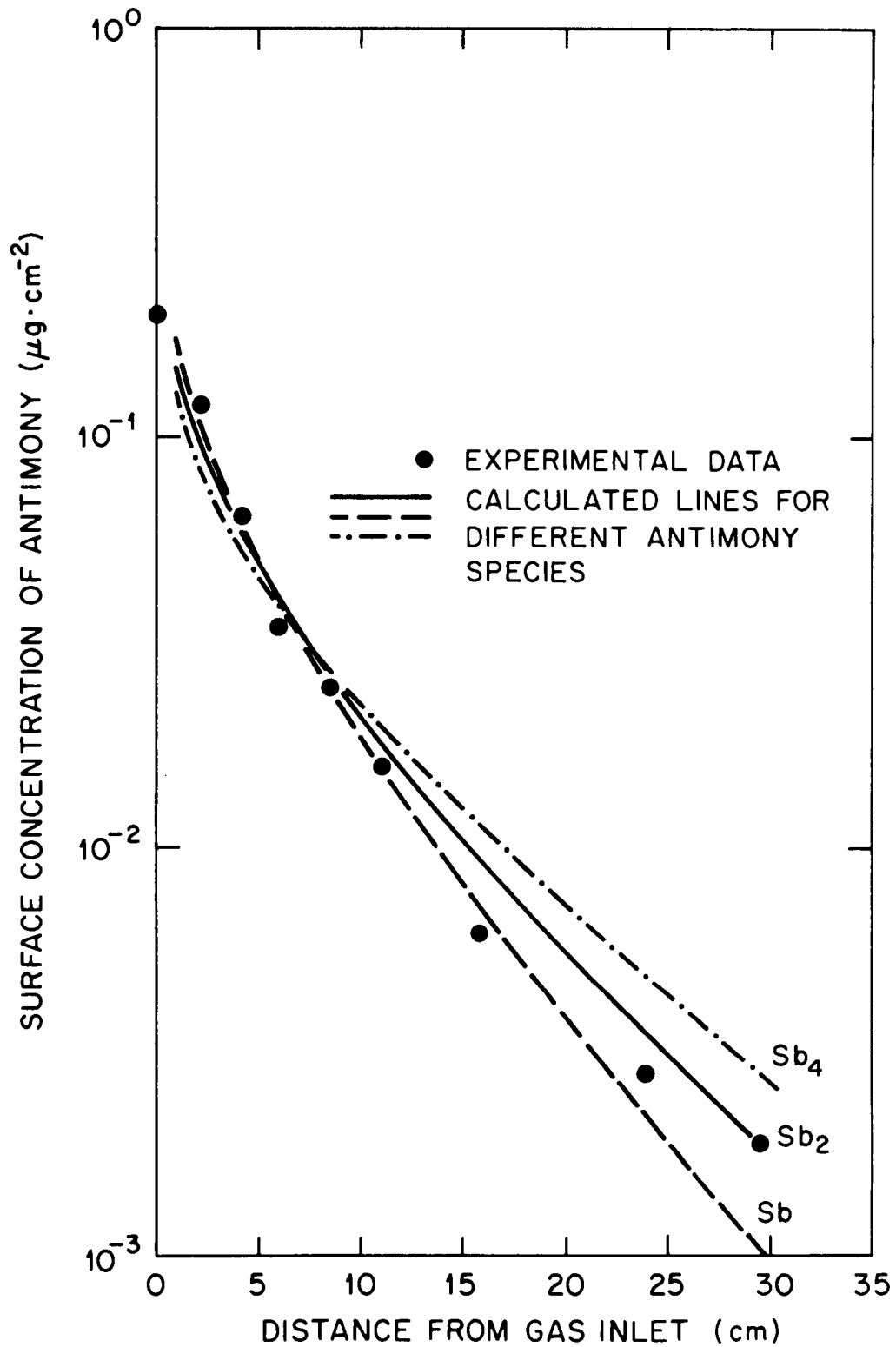


Fig. 12. Antimony deposition profiles from measured and calculated values for test HBU-11.

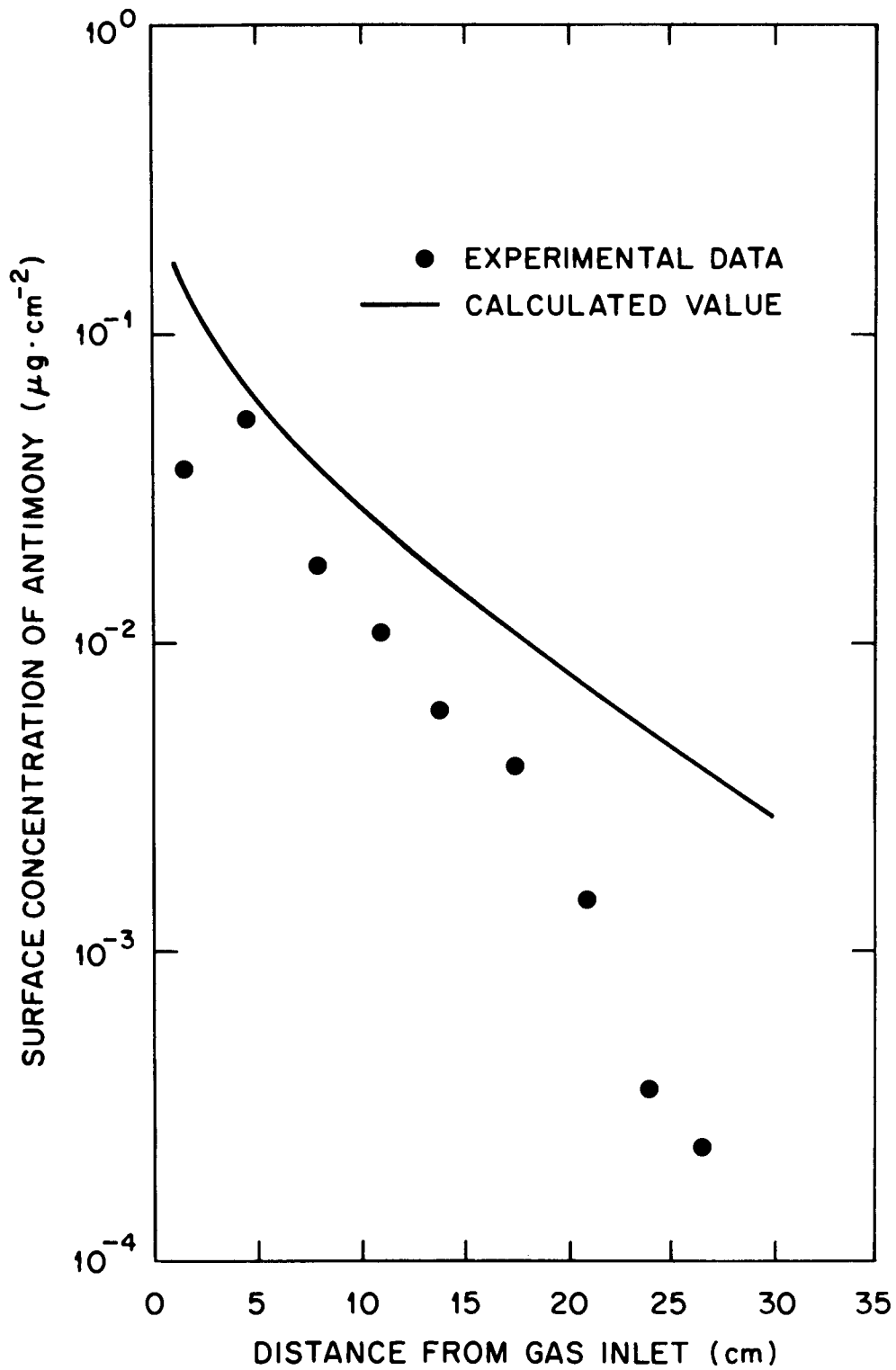


Fig. 13. Antimony deposition profiles from measured and calculated values for test HI-1.

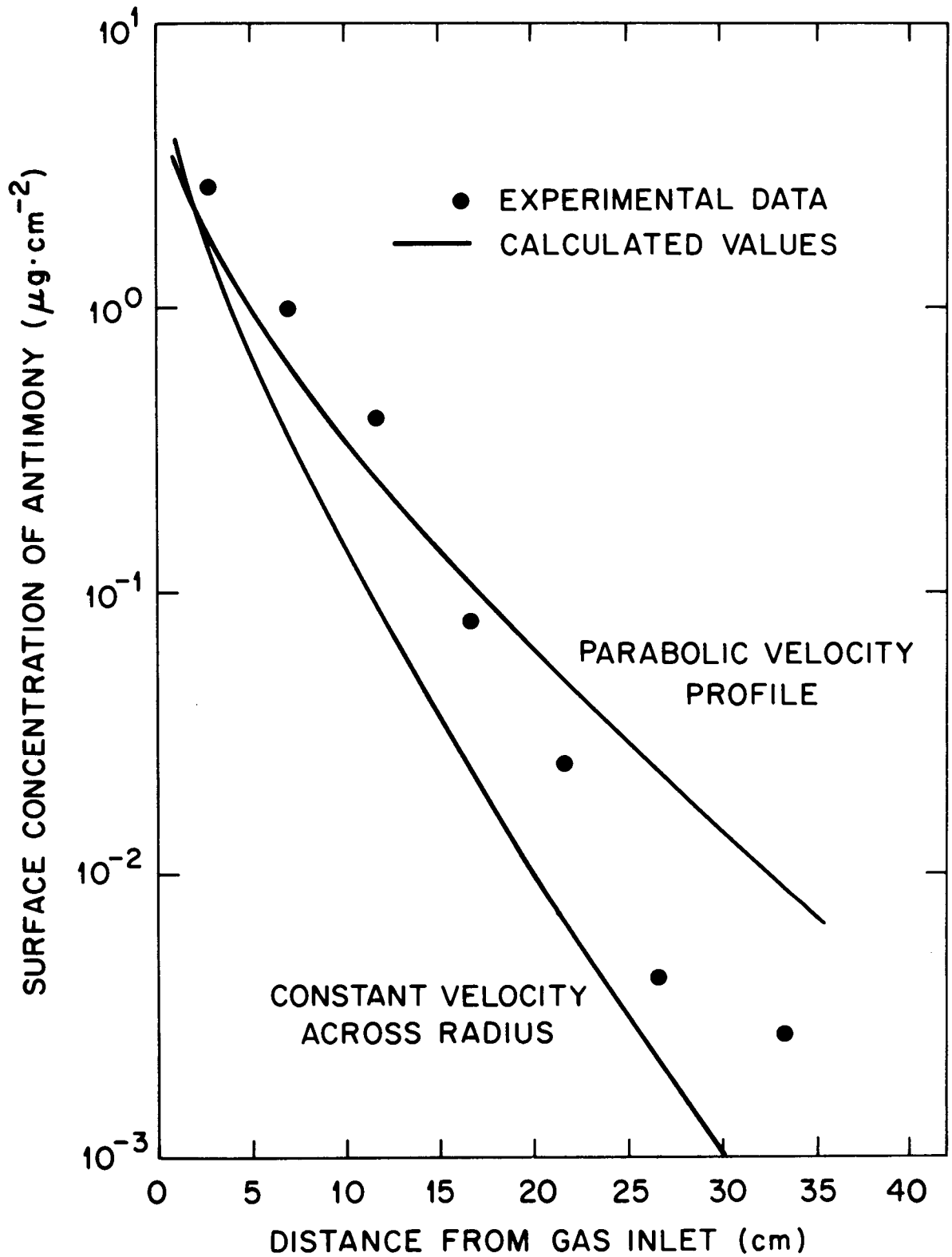


Fig. 14. Antimony deposition profiles from measured and calculated values for test HI-2.

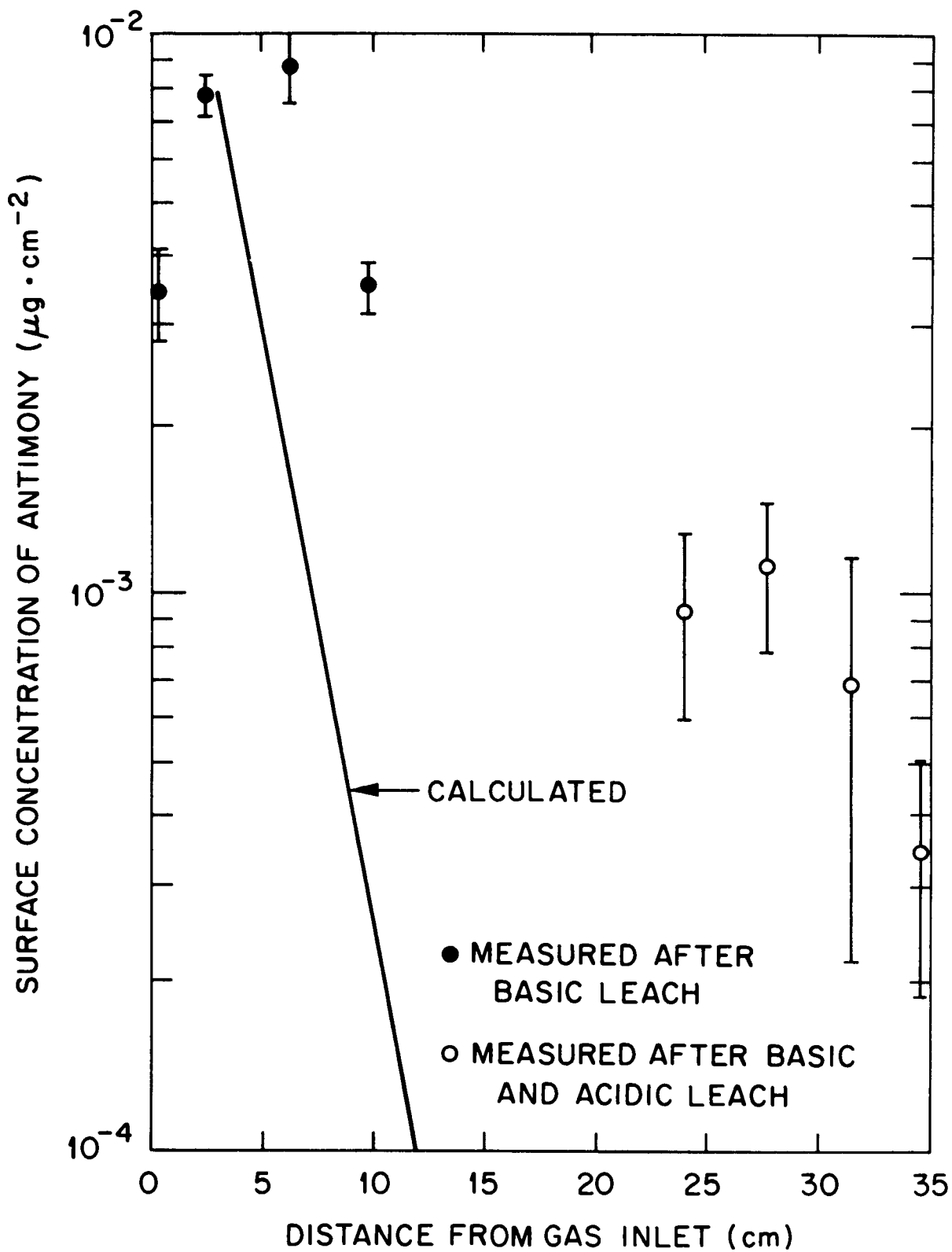


Fig. 15. Antimony deposition profiles from measured and calculated values for test HI-5.

<u>Test No.</u>	<u>Antimony leaving the TGT (μg)</u>	
	<u>Measured</u>	<u>Calculated</u>
HBU-11	0.028	0.041
HI-1	Not measured	0.061
HI-2	0.111	0.098

The calculations agree moderately well with the measured data, considering the simplicity of the model. The discrepancies may be explained in two ways:

The HBU-11 antimony profile was measured immediately after its formation, while the HI-1 and HI-2 profiles were obtained after a basic leach and sometimes after an acid leach as well. Thus antimony could be lost by leaching from the TGT in HI-1 and HI-2 before it was detected.

Secondly, the fuel in HBU-11 reached 1200°C only, and Zircaloy oxidation would have produced a slow, steady stream of hydrogen. The fuel in HI-1 reached 1400°C, and in HI-2 it reached 1700°C; in both cases hydrogen was evolved rapidly in the early stages of the test. Hydrogen increases the diffusion coefficient of antimony in the flowing gas, causing a deposition profile steeper than that from the average gas composition.

Figure 15 shows that the calculated antimony profile in HI-5 is very different from the measured one. The only explanation is that argon was inadvertently used as the bulk gas instead of helium, but this seems very unlikely. Until this discrepancy is resolved, calculation of antimony profiles must be considered a doubtful process.

Antimony was assumed to be the main species in the diffusion calculations. Antimony vapor is an equilibrium mixture of Sb, Sb₂, and Sb₄; the Sb₂ and Sb₄ predominate over condensed-phase antimony at TGT temperatures, but Sb₂ would be the major species at the very low antimony partial pressures in the fission product release tests. Figure 12 shows that the calculated deposition profile is insensitive to the choice of antimony species.

The gas in the TGT is hotter than the deposition surfaces, with a temperature difference varying from ~70 C° for argon-based gas to ~15 C° for helium-based gas, depending on the gas thermal diffusivity. The temperature difference has little effect on the deposition profile; a variation of 0-65 C° causes <10% change in surface concentrations or in the quantity of antimony escaping from the TGT.

If the gas flow in the TGT is turbulent, it increases the apparent diffusivity of antimony in the gas mixture and flattens the parabolic gas velocity profile. Figure 14 illustrates this flattening effect. Also, with turbulent gas flow the deposition profile is much steeper, and less antimony escapes from the thermal gradient tube [0.0035 μg (calculated) versus 0.11 μg (measured)]. This effect is shown in Fig. 15. This implies that flow in the thermal gradient tube is laminar.

Reynolds numbers in the thermal gradient tube tests were usually in the range of a few hundred. For instance, for test HI-1 the Reynolds number increased from ~250 at the TGT inlet to ~600 at the TGT outlet — well below the turbulent transition region around 2000.

In all of the four experiments, antimony was observed to deposit at temperatures much higher than those for which a pure condensed antimony phase is stable.¹⁶ Apparently, some process reduced the chemical potential of antimony on the platinum surface.

Antimony diffuses into solid platinum, and if this process is rapid compared to the rate of arrival of antimony from the gas, then antimony will deposit and not reevaporate. Appendix D quantifies the idea of "rapid" by determining the minimum values for the antimony-into-platinum diffusion coefficients required to reproduce the observations. In Fig. 16, these values are plotted as a function of temperature for HBU-11, HI-1, and HI-2.

The actual diffusion coefficient for antimony in platinum has not been determined; however, tellurium is the adjacent element in the periodic table and forms similar intermetallics with platinum, so its diffusivity should be similar to that of antimony. An experimental range for diffusion coefficients of tellurium in platinum (see Appendix E) has been plotted in Fig. 16 for comparison.

It can be seen in Fig. 16 that at temperatures $>500^{\circ}\text{C}$, solid-state diffusion alone is not sufficient to cause the condensation of antimony. The extra driving force for deposition may be the formation of platinum antimony compounds such as PtSb_2 . Appendix F estimates the stability of such a compound. If compound formation reduces the activity of antimony in platinum by an activity coefficient of γ , D_{min} is reduced to $\gamma^2 D_{\text{min}}$. It is thus plausible that a combination of compound formation and diffusion drives the deposition of antimony in the hotter areas of the thermal gradient tube where pure antimony is not stable.

Figure 16 shows that antimony also deposited on the gold thermal gradient tube of HBU-11, at high temperatures. The enthalpy of formation of AuSb_2 has been measured as -5 kJ/mol Sb at 450°C (Ref. 17), so compound formation is a very minor process. Diffusion of antimony in gold is more rapid than that in platinum at the same temperature (qualitatively because gold melts at 1340 K and platinum at 2040 K). Figure 16 shows the values for diffusion coefficients of antimony in gold for comparison with the HBU-11 results.¹⁸

To summarize, a combination of gas-phase diffusion, compound formation, and solid-phase diffusion can account for the behavior of antimony on platinum, but not for its deposition on gold, with moderate confidence. The evidence indicates an unknown extra process which encourages antimony to remain on gold surfaces.

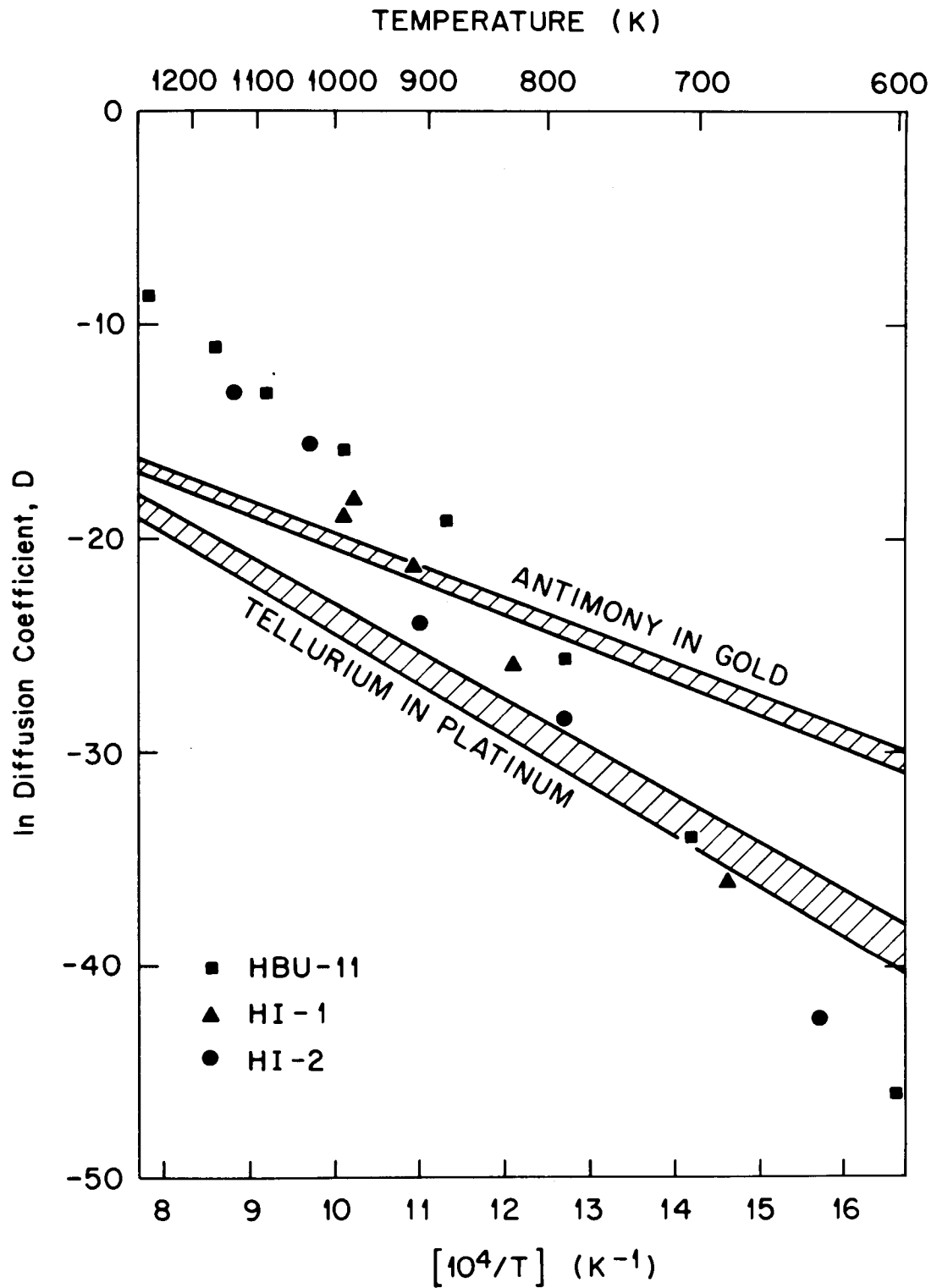


Fig. 16. Comparison of the diffusion coefficients for antimony in gold and platinum with the minimum values necessary for tests HI-1, HI-2, and HBU-11.

9. POSSIBLE TELLURIUM ANALYSES

Data on tellurium behavior is needed to calculate fractional releases from the fuel and to provide clues as to the chemical form of tellurium releases.

Direct gamma spectroscopy is impossible, because radioactive tellurium isotopes are either short-lived or emit gamma rays with low abundance and low energy. Colorimetric techniques are not sensitive enough (e.g., the method of Busev et al.¹⁹ requires $>10 \mu\text{g}$). Spark-source mass spectrometry has been used because the sensitivity is good, and the precision is adequate (a factor of 2 is quoted, but results seem better than this). However, representative samples are very difficult to obtain by scraping the TGT surface with a graphite electrode, especially since the tellurium diffuses into platinum at high temperatures.

In an effort to obtain more tellurium data, a new procedure was developed. The procedure, discussed in Appendix G, involves the separation by precipitation of tellurium from platinum and strong gamma-emitting nuclides such as ^{134}Cs and ^{137}Cs . Tellurium is finally determined by neutron activation to ^{131}I on ion-exchange resin. The procedure was developed using $^{129\text{m}}\text{Te}$ as a tellurium tracer.

10. CONCLUSIONS

1. In this experimental system, the cesium profile was governed by Cs-S-O species; the sulfur was a contaminant in the furnace ceramics and will be absent in reactors.
2. Less than 0.5% of the iodine released from the fuel was released in a penetrating form (perhaps I_2 or CH_3I). The remainder was present as an involatile species, probably CsI.
3. Cesium iodide, the presumed form of the released iodine in the HI series of tests, deposited on platinum with apparent mass transfer coefficients ranging from 1.9 to $5.8 \text{ cm}\cdot\text{s}^{-1}$.
4. Silver was released from fuel as elemental vapor; after condensation to an aerosol, it was deposited on filters, with some particle deposition in the TGT.
5. Antimony was released as Sb_2 and reacted rapidly and irreversibly with Pt or Au thermal gradient tube liners by compound formation and diffusion. The a priori calculations of antimony behavior in the TGT have been partially successful.
6. Tellurium has been quantitatively separated from platinum during laboratory tests, in a form suitable for neutron activation. This makes possible precise tellurium analyses in future fission product release tests.

11. ACKNOWLEDGMENTS

I would like to thank M. F. Osborne, R. A. Lorenz, J. L. Collins, J. R. Travis, and C. S. Webster, who performed the fission product release tests at ORNL, and with whom I discussed much of the content of this report. T. B. Lindemer and R. P. Wichner also helped with fruitful discussions, and M. F. Osborne, R. P. Wichner, and B. C. Drake completed production of this report after I returned to Britain.

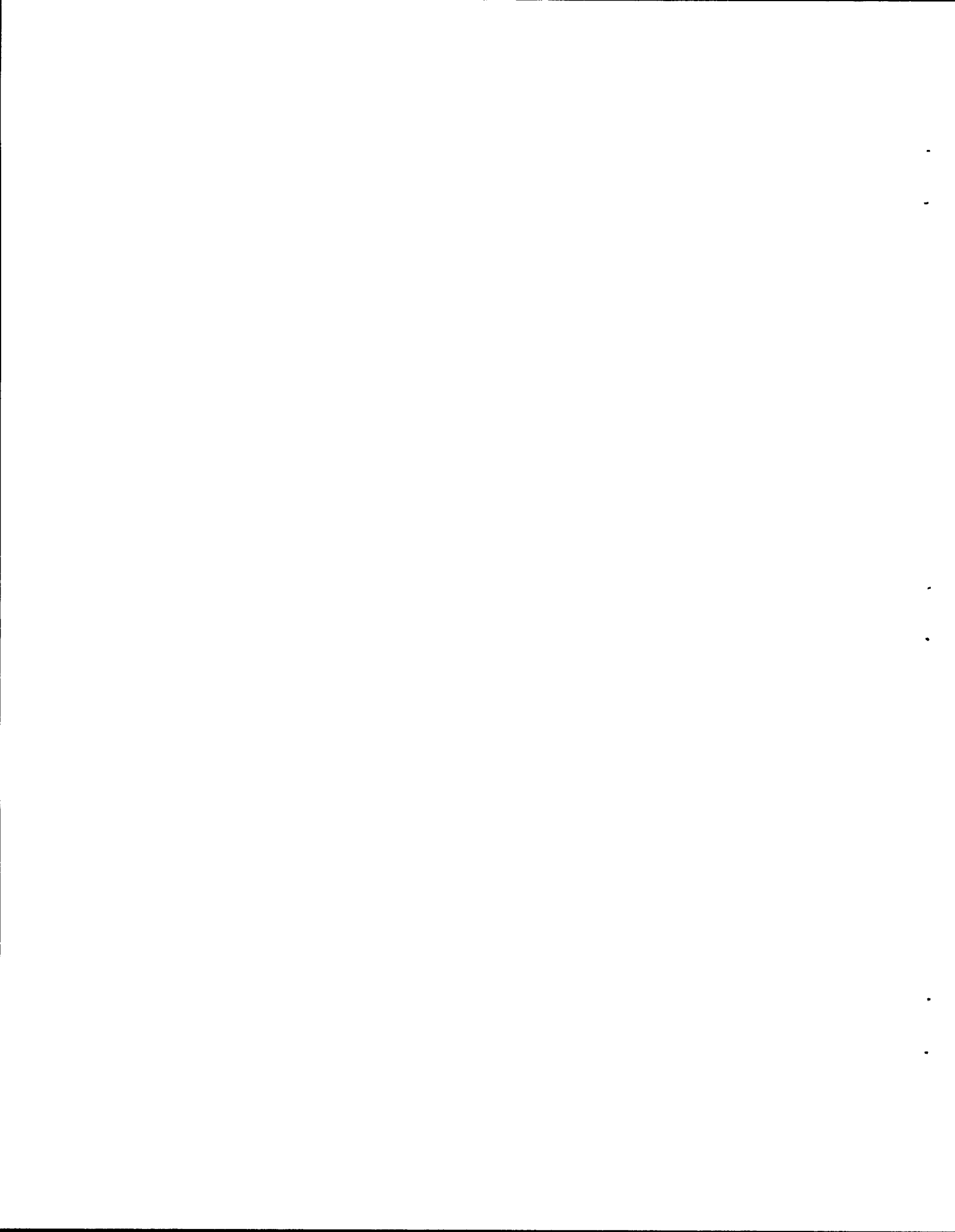
I wish to thank the United Kingdom Atomic Energy Authority, who supported me at ORNL under an administrative agreement with the U. S. Nuclear Regulatory Commission.

12. REFERENCES

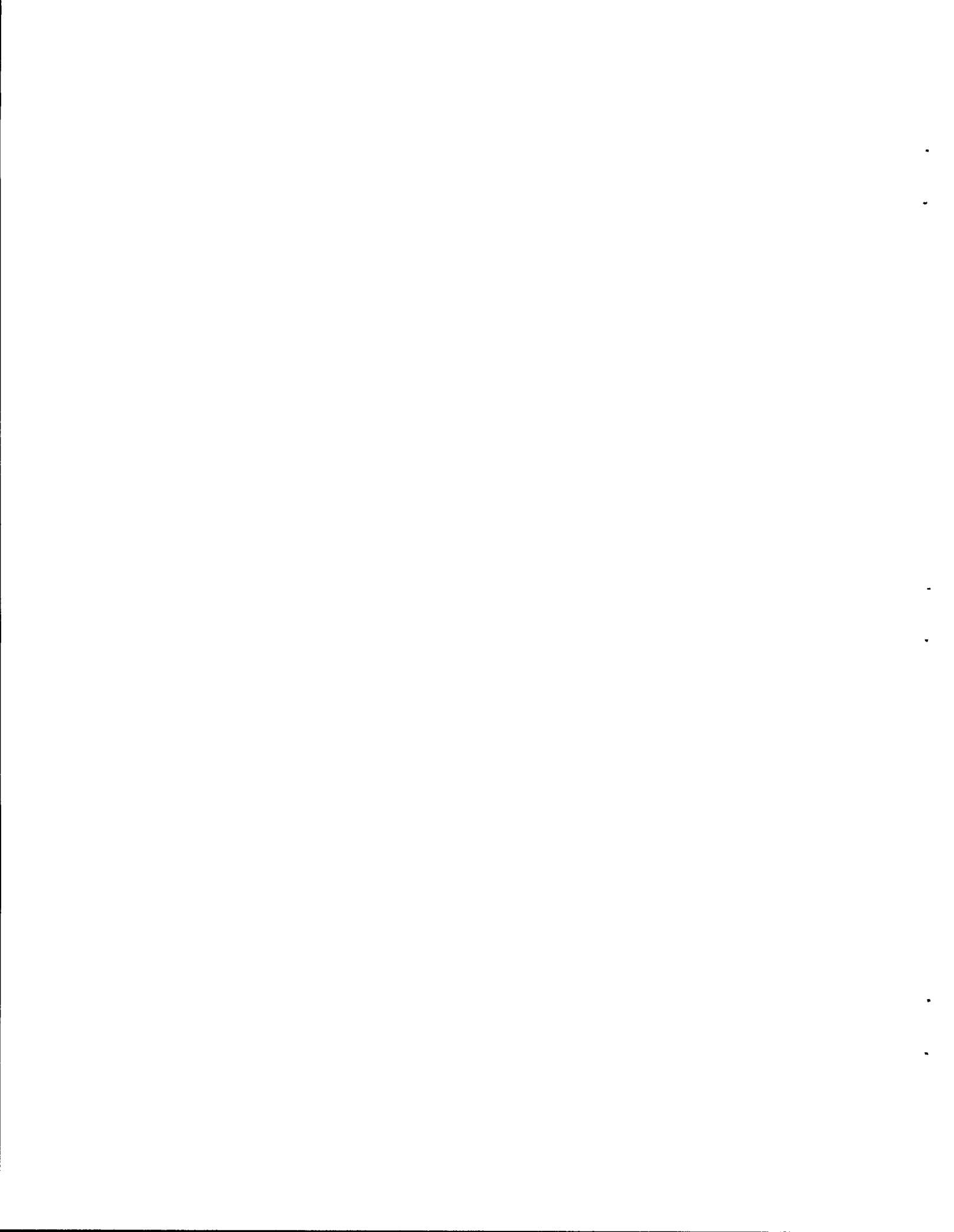
1. M. F. Osborne, R. A. Lorenz, J. R. Travis, and C. S. Webster, Data Summary Report for Fission Product Release Test HI-1, NUREG/CR-2928 (ORNL/TM-8500) December 1982.
2. M. F. Osborne, R. A. Lorenz, J. R. Travis, C. S. Webster, and K. S. Norwood, Data Summary Report for Fission Product Release Test HI-2, NUREG/CR-3171 (ORNL/TM-8667), February 1984.
3. M. F. Osborne, R. A. Lorenz, K. S. Norwood, J. R. Travis, and C. S. Webster, Data Summary Report for Fission Product Release Test HI-3, NUREG/CR-3335 (ORNL/TM-8793), March 1984.
4. M. F. Osborne, J. L. Collins, R. A. Lorenz, K. S. Norwood, J. R. Travis, C. S. Webster, Data Summary Report for Fission Product Release Test HI-4, NUREG/CR-3600 (ORNL/TM-9011), June 1984.
5. M. F. Osborne, J. L. Collins, R. A. Lorenz, K. S. Norwood, J. R. Travis, and C. S. Webster, Data Summary Report for Fission Product Release Test HI-5, NUREG/CR-4037 (ORNL/TM-9437), in preparation.
6. M. F. Osborne, J. L. Collins, R. A. Lorenz, J. R. Travis, and C. S. Webster, Design, Construction, and Testing of a 2000°C Furnace and Fission Product Collection System, NUREG/CR-3715 (ORNL/TM-9135), September 1984.
7. J. L. Collins, M. F. Osborne, R. A. Lorenz, K. S. Norwood, J. R. Travis, and C. S. Webster, Observed Behavior of Cesium, Iodine, and Tellurium in the ORNL Fission Product Release Program, NUREG/CR-3930 (ORNL/TM-9316), in publication.
8. P. Lebeau, Ann. Chim. Phys. Series 8, 6, 422-32 (1950).
9. T. B. Lindemer, T. M. Besmann, and C. E. Johnson, "Thermodynamic Review and Calculations — Alkali-Metal Oxide Systems with Nuclear Fuels, Fission Products, and Structural Materials," J. Nucl. Mater. 100, 1-3 (1981).

10. M. D. Scheer and J. Fine, J. Chem. Phys. 36, 1647 (1962).
11. V. Dietz, J. Chem. Phys. 4, 575-80 (1936).
12. I. Barin and O. Knacke, Thermochemical Properties of Inorganic Substances, Springer-Verlag, New York, 1973, p. 254.
13. N. A. Lange, ed., Handbook of Chemistry, 9th Ed., McGraw-Hill, New York, 1956, p. 1426.
14. R. Hultgren et al., Selected Values of the Thermodynamic Properties of the Elements, American Society for Metals, Metals Park, OH, 1973, p. 21.
15. R. A. Lorenz, J. L. Collins, A. P. Malinauskas, O. L. Kirkland, and R. L. Towns, Fission Product Release from Highly Irradiated LWR Fuel, NUREG/CR-0722 (ORNL/NUREG/TM-287/R2), February 1980.
16. R. Hultgren et al., Selected Values of the Thermodynamic Properties of the Elements, American Society for Metals, Metals Park, Ohio, 1973, p. 446.
17. R. Hultgren et al., Selected Values of the Thermodynamic Properties of Binary Alloys, American Society for Metals, Metals Park, Ohio, 1973, p. 314.
18. C. Herzig and T. Heumann, Z. Naturforsch. A, 27(A), 613-17 (1972).
19. A. I. Busev, V. G. Tiptsova, and V. M. Ivanov, Handbook of the Analytical Chemistry of Rare Elements, Ann Arbor-Humphrey Science, 1970, p. 388 et seq..
20. R. B. Bird et al., Transport Phenomena, J. Wiley and Sons, Inc., New York, 1960, p. 505.
21. J. C. Bailar et al., Comprehensive Inorganic Chemistry, Vol. 2, Pergamon Press, 1973, p. 555.
22. A. Gmelin, Handbuch der Anorganischen Chemie: Antimon B, 1949, p. 69.
23. R. C. Weast, CRC Handbook of Chemistry and Physics, 64th Ed., 1983, p. B-70.
24. R. B. Bird et al., Transport Phenomena, J. Wiley and Sons, Inc., New York, 1960, p. 571.
25. J. Crank, The Mathematics of Diffusion, Oxford Clarendon Press, Oxford, England, 1956.

26. J. Askill, Tracer Diffusion Data for Metals, Alloys, and Simple Oxides, IFI/Plenum Press, New York, 1970.
27. W. G. Moffatt, The Handbook of Binary Phase Diagrams, GE, 1978.
28. M. Hansen and K. Anderko, Constitution of Binary Alloys, 2nd Ed., McGraw-Hill, New York, 1958.
29. A. I. Vogel, A Textbook of Quantitative Inorganic Analysis, 3rd Ed., Longmans, 1961, p. 508.
30. L. C. Bate and J. R. Stokeley, Determination of Iodine-129 in Mixed Fission Products by Neutron Activation Analysis, ORNL/TM-7449, Oak Ridge National Laboratory, Oak Ridge, Tenn., October 1980.
31. U. Schindewolf, "Selenium and Tellurium Content of Stony Meteorites by Neutron Activation," Geochim. Cosmochim. Acta 19, 134 (1960).



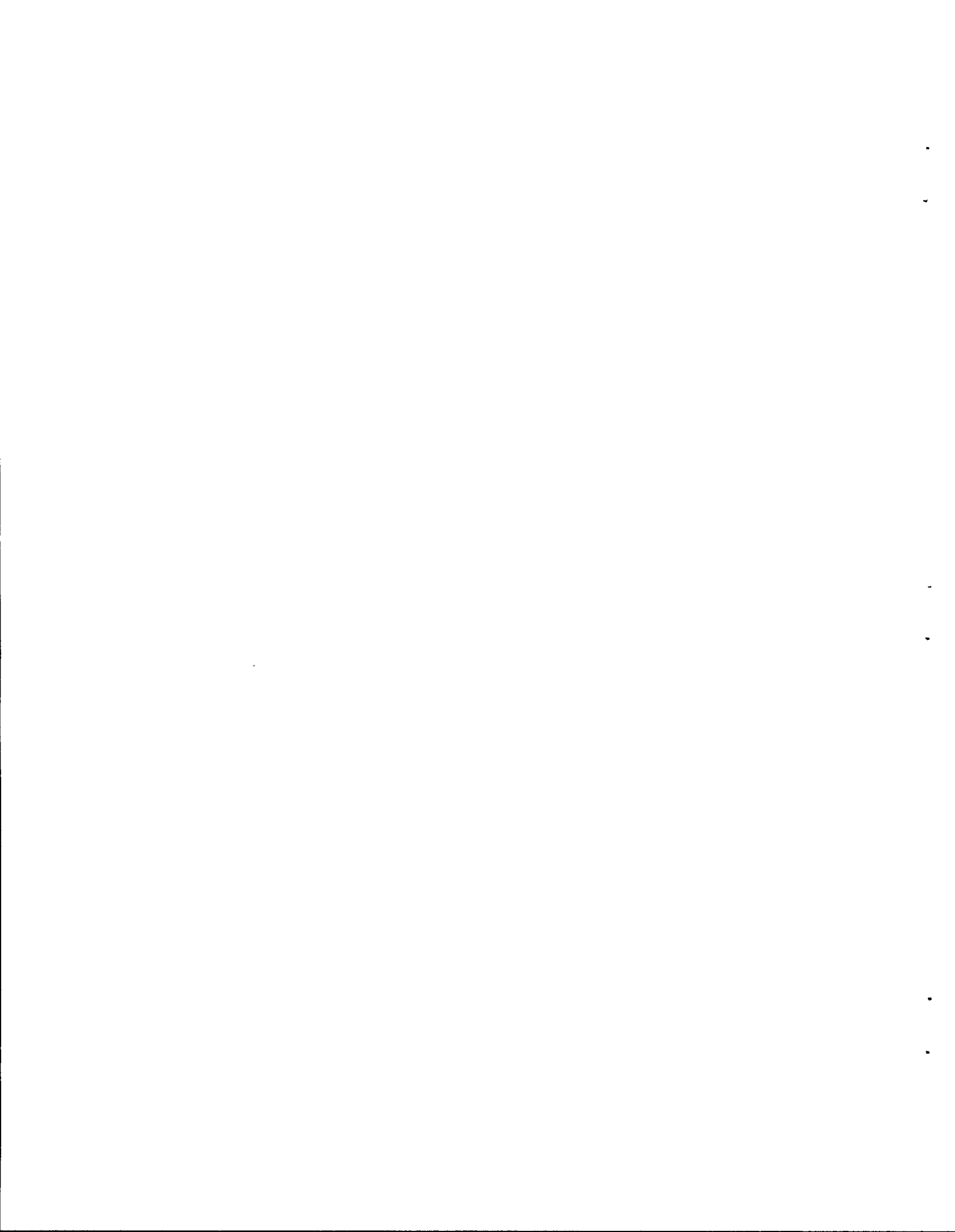
APPENDIXES



APPENDIX A. APPLICATION OF RAOULT'S LAW TO CsI TGT PROFILE

Iodine was deposited on the TGT at temperatures above the condensation temperature of CsI. However, iodine always condenses in the presence of excess cesium, implying that a solid solution of CsI in another compound (CsX) may form that reduces the vapor pressure of CsI.

For instance, at the inlet to the TGT in test HI-3, the platinum surface had a temperature of 740°C. At this temperature, cesium iodide has a saturated vapor pressure of 50 to 230 Pa (using values from refs. 12 and 13 as bounds). The TGT section analyzed contained a deposit of 3100 µg Cs and 56 µg I, so the approximate mole ratio (CsX/CsI) was 52. Raoult's Law gives the saturated vapor pressure of CsI above a solid solution of this composition as 0.96 to 4.4 Pa. Since this is less than the partial pressure of CsI in the gas (10 Pa), CsI would deposit; this is the case for all sections of the TGT, and helps to explain the observed peak broadening.



APPENDIX B: CALCULATION OF DIFFUSION COEFFICIENT
FOR ANTIMONY IN A MIXED GAS

An empirical correlation exists between the diffusion coefficient of one gaseous species in another and their critical constants:²⁰

$$pD_{AB} = a \cdot T^b \cdot (P_A P_B)^{1/3} (T_A T_B)^{5/12 - b/2} (1/M_A + 1/M_B)^{1/2},$$

where

- p = pressure (Pa),
- P_A = critical pressure of species A (Pa),
- T = temperature (K),
- T_A = critical temperature of species A ($^{\circ}$ C),
- M_A = molecular weight of species A (amu),
- D_{AB} = interdiffusion coefficient of A and B ($\text{cm}^2 \cdot \text{s}^{-1}$),
- a = 2.745×10^{-4} for nonpolar gas pairs, 3.640×10^{-4} for water and a nonpolar gas,
- b = 1.823 for nonpolar gas pairs, 2.334 for water and a nonpolar gas.

The critical constants of water, hydrogen, helium, and argon have been measured, but empirical correlations are needed to determine those of antimony.

The critical temperature is about $1.5 \times$ boiling point, or $1.5 \times 1635^{\circ}\text{C} = 2589^{\circ}\text{C}$, for antimony. The boiling point of antimony has been taken as 1635°C ,²¹ which also lies at the upper end of the boiling point range cited in Gmelin.²² A more recent value is 1750°C , which would affect calculated values of the diffusion coefficient by $<5\%$.²³ The major antimony species in the fission product release experiments is probably Sb_2 ; the molar volume of Sb_2 at the boiling point is $2 \times 121.75/6.68 = 36.5 \text{ cm}^3$, assuming the density of antimony changes little from room temperature to the boiling point. The critical volume is $36.5/0.376 = 97 \text{ cm}^3$. Since the critical constants obey the approximate relationship $p_c V_c = 0.267 RT_c$, $p_c = 6.47 \times 10^7 \text{ Pa}$ for antimony.

<u>Species</u>	<u>Molecular weight (amu)</u>	<u>Critical temperature ($^{\circ}$C)</u>	<u>Critical pressure (Pa)</u>
H_2	2.02	-240	1.3×10^6
H_2O	18.02	374	2.18×10^7
Ar	39.95	-122	4.9×10^6
He	4.00	-267.7	2.3×10^5
Sb_2	243.50	2587	6.5×10^7

Using these data, the empirical correlations yield the following values for Sb_2 diffusion coefficients at $1000^\circ C$ and $10^5 Pa$:

carrier gas	H_2	He	H_2O	Ar
D ($cm^2 \cdot s^{-1}$)	6.2	6.2	1.6	1.1

For an ideal gas mixture, the diffusion coefficient of a species is exactly related to its diffusion coefficient in the separate gases by:²⁴

$$\frac{1-x_1}{D_{1m}} = \sum_{j=2}^n \frac{x_j}{D_{1j}},$$

where

x_j = mole fraction of gas j in the mixture,

D_{1j} = diffusion coefficient of gas 1 in gas j ,

D_{1m} = diffusion coefficient of gas 1 in the mixture.

For instance, while the fuel specimen was at maximum temperature in HI-2, the average gas composition was 0.51 hydrogen, 0.24 water, 0.25 argon (in mole-fraction units), so

$$\frac{1}{D_{Sb_2}} = \frac{0.51}{6.2} + \frac{0.24}{1.6} + \frac{0.25}{1.1},$$

and D_{Sb_2} in HI-2 at $1000^\circ C$ was $2.2 cm^2 \cdot s^{-1}$.

APPENDIX C. CALCULATION OF ANTIMONY DEPOSITION PROFILE IN TGT

A rigorous calculation of deposition in the thermal gradient tube requires that the equations of continuity, motion, and energy be solved for five variables at each point in the gas: temperature, pressure, axial and radial velocities, and antimony concentration. Some simplifying assumptions were made for the calculations reported here:

1. The gas has the parabolic velocity profile across the radius of the tube typical of laminar flow of a viscous fluid.
2. The linear velocity of the gas decreases with temperature only because the density increases. There is no motion of the gas radially.

These assumptions determine the flow pattern of the bulk gas, and the diffusion of antimony can easily be superimposed on this pattern. A simple computer program was written in HPL (Hewlett-Packard Programming Language) to carry out the diffusion calculations on an HP-9825A in the group. The program employs established principles and will be described briefly here.

The thermal gradient tube was discretised into annular volumes and the diffusion and transport equations written for each volume; Fig. C.1 illustrates this and the use of subscripts in the equations that follow:

$$\text{flux of antimony into annulus} = S_{n-1/2,m-1/2} \cdot B_n \text{ g} \cdot \text{s}^{-1} ,$$

where

$$B_n = \text{bulk gas flow in annulus } n, \text{ g} \cdot \text{s}^{-1} \text{ (} B_n \text{ is constant along the thermal gradient tube length),}$$

$$S_{n-1/2,m-1/2} = \text{concentration of antimony in annulus directly upstream, g Sb} \cdot (\text{g bulk gas})^{-1} .$$

$$\text{flux of antimony leaving annulus} = S_{n-1/2,m+1/2} \cdot B_n \text{ g} \cdot \text{s}^{-1} ,$$

$$\text{concentration of antimony at center of annulus} =$$

$$\rho_{n-1/2,m+1/2} \cdot S_{n-1/2,m+1/2} \text{ (g} \cdot \text{cm}^{-3} \text{) ,}$$

$$\rho_{n-1/2,m+1/2} = \text{density of bulk gas at center of annulus, g} \cdot \text{cm}^{-3} \text{ (} \rho \text{ depends on } T_{n-1/2,m+1/2} \text{),}$$

$$\text{concentration gradient across outer curved face} =$$

$$\frac{\rho_{n+1/2,m+1/2} \cdot S_{n+1/2,m+1/2} - \rho_{n-1/2,m+1/2} \cdot S_{n-1/2,m+1/2}}{r_{n+1/2} - r_{n-1/2}}$$

TYPICAL ANNULAR SUBDIVISION OF TGT

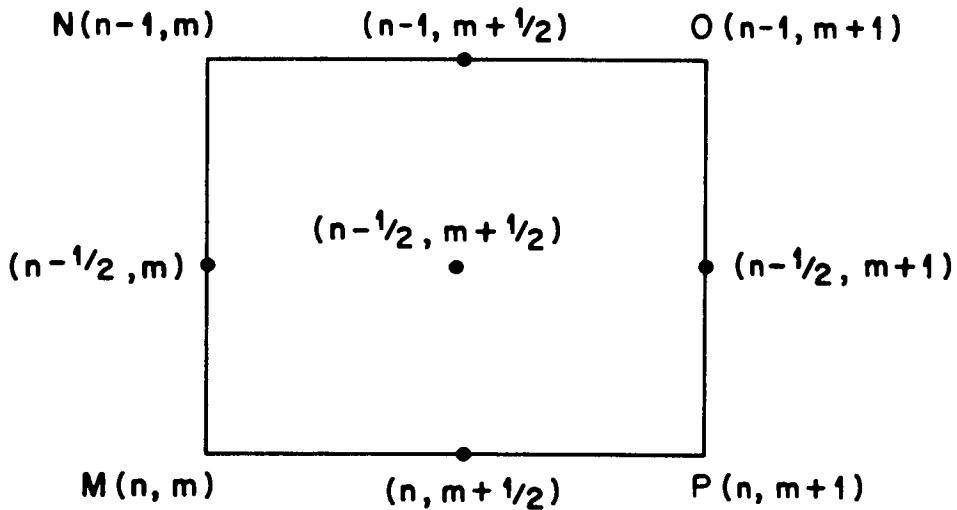
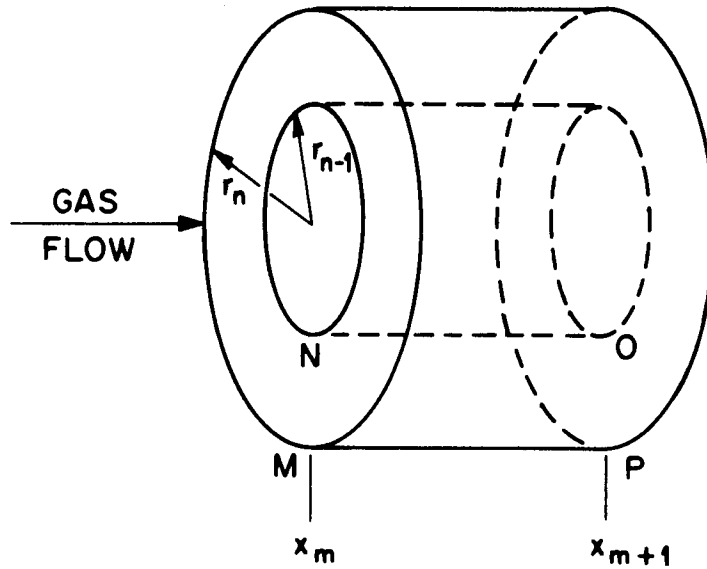


Fig. C.1. Diagram of discretisation employed in antimony diffusion computer program.

where

$r_{n-1/2}$ = radius of "center" of annulus n.

This concentration gradient is multiplied by $C_{n,m+1/2}$ [cm^2 , the area of the outer curved face, found by $2\pi r_n (x_{m+1} - x_m)$] and $D_{n,m+1/2}$ ($\text{cm}^2 \cdot \text{s}^{-1}$, the diffusion coefficient for antimony in the bulk gas, see Appendix C) to give the flux of antimony across the curved face in $\text{g} \cdot \text{s}^{-1}$.

Combining the antimony fluxes across all the faces of annulus n and conserving the mass of antimony, we have:

$$M_{1,n} S_{n-3/2,m+1/2} + M_{2,n} S_{n-1/2,n+1/2} + M_{3,n} S_{n+1/2,m+1/2} = B_n S_{n-1/2,m-1/2} ,$$

where

$$M_{1,n} = \frac{- D_{n-1,m+1/2} \cdot C_{n-1,m+1/2} \cdot \rho_{n-3/2,m+1/2}}{r_{n-1/2} - r_{n-3/2}} ,$$

$$M_{2,n} = B_n + \frac{D_{n,m+1/2} \cdot C_{n,m+1/2} \cdot \rho_{n-1/2,m+1/2}}{r_{n+1/2} - r_{n-1/2}} + \frac{D_{n-1,m+1/2} \cdot C_{n-1,m+1/2} \cdot \rho_{n-1/2,m+1/2}}{r_{n-1/2} - r_{n-3/2}} ,$$

$$M_{3,n} = \frac{- D_{n,m+1/2} \cdot C_{n,m+1/2} \cdot \rho_{n+1/2,m+1/2}}{r_{n+1/2} - r_{n-1/2}} .$$

The boundary condition on the innermost annulus is that there is no antimony flux across its interior boundary. The other boundary condition is that the antimony concentration at the wall is zero. These are expressed mathematically by the following expressions:

inner condition:

$$\left(B_1 + \frac{D_{1,m+1/2} \cdot C_{1,m+1/2} \cdot \rho_{0,m+1/2}}{r_{3/2} - r_0} \right) S_{1/2,m+1/2} - \left(\frac{D_{1,m+1/2} \cdot C_{1,m+1/2} \cdot \rho_{3/2,m+1/2}}{r_{3/2} - r_0} \right) S_{3/2,m+1/2} = B_1 S_{1/2,m-1/2} ,$$

outer condition:

$$\begin{aligned} & \left(\frac{-D_{N-1,m+1/2} \cdot C_{N-1,m+1/2} \cdot \rho_{N-3/2,m+1/2}}{r_{N-1/2} - r_{N-3/2}} \right) S_{N-3/2,m+1/2} \\ & \left(B_N + \frac{D_{N,m+1/2} \cdot C_{N,m+1/2} \cdot \rho_{N-1/2,m+1/2}}{r_N - r_{N-1/2}} + \right. \\ & \left. \frac{D_{N-1,m+1/2} \cdot C_{N-1,m+1/2} \cdot \rho_{N-1/2,m+1/2}}{r_{N-1/2} - r_{N-3/2}} \right) S_{N-1/2,m+1/2} \\ & = B_N S_{N-1/2,m-1/2} \end{aligned}$$

These equations form a matrix equation that can be solved by Gaussian elimination:

$$\tilde{M} \cdot \vec{S}_{m+1/2} = \vec{BS}_{m-1/2},$$

where

$$\begin{aligned} \tilde{M} &= \text{tridiagonal transport matrix,} \\ \vec{BS}_{m-1/2} &= \text{vector of antimony fluxes from previous axial position,} \\ \vec{S}_{m+1/2} &= \text{vector of antimony concentrations at new axial position.} \end{aligned}$$

For a parabolic velocity profile in a tube of radius r_0 , the fraction of the volume flow rate passing through the annulus with inner radius a_0 and outer radius b_0 is

$$(2b^2 - b^4) - (2a^2 - a^4).$$

In the program, these fractions are weighted according to gas density (which varies with temperature from annulus to annulus) to provide B_n , the bulk flow rate in $\text{g} \cdot \text{s}^{-1}$ in annulus n .

In the program, the TGT was divided into ten annuli with radial cross-sections of equal area. Concentration profiles set up by diffusion are roughly parabolic, but with this subdivision they appear linear to the mathematical solution technique, which then gives more accurate answers.

The program analyzes the thermal gradient tube by 0.1-cm lengths; decreasing the step length to 0.05 cm changes the calculated antimony profile by <2%.

The model was set up to conserve the mass of antimony; in practice, it conserves antimony to better than 2.3 parts in 10^6 over a 35-cm thermal gradient tube.

APPENDIX D. ESTIMATION OF THE MINIMUM DIFFUSION COEFFICIENT FOR
ANTIMONY IN PLATINUM FROM THERMAL GRADIENT TUBE DATA

Antimony deposits in the thermal gradient tube even when its partial pressure in the gas is less than the saturated vapor pressure of elemental antimony. Some process must remove antimony from the platinum surface — chemical reaction or diffusion.

The concentration of diffusing antimony (C) depends on time (t) and depth into the platinum (x) when the flux to the surface is constant:²⁵

$$C = \frac{F}{(\pi D)^{1/2}} \int_0^t \exp\left\{-\frac{x^2}{4D(t-\tau)}\right\} \cdot \frac{d\tau}{(t-\tau)^{1/2}},$$

where

F = flux of antimony to the surface ($\text{atoms} \cdot \text{cm}^{-2} \cdot \text{s}^{-1}$),
 D = diffusion coefficient ($\text{cm}^2 \cdot \text{s}^{-1}$).

The antimony concentration at the surface ($x = 0$) is:

$$C \text{ (atoms} \cdot \text{cm}^{-3}\text{)} = \frac{2F}{(\pi D)^{1/2}} \cdot t^{1/2}.$$

F can be estimated from measurements on the thermal gradient tube. The partial pressure of antimony in the flowing gas defines the maximum surface concentration; t is taken as the time while the fuel specimen was at maximum temperature. Then the diffusion coefficient for antimony in platinum must be larger than D_{\min} where:

$$D_{\min} = \frac{4F^2 t}{\pi C^2}.$$

For example, gamma spectrometry on samples from HI-2 showed that 19.29 μg antimony entered the thermal gradient tube and 0.1135 μg left it while 1.12 mol of gas flowed through.² This corresponds to a partial pressure of 4.0×10^{-3} Pa at inlet and 2.1×10^{-5} Pa at outlet; these figures are approximate, because antimony vapor is an equilibrium mixture of Sb_4 , Sb_2 , and Sb . The partial pressure of antimony along the thermal gradient tube probably declines exponentially, like the surface concentration.

The antimony sample from the inlet of the TGT in HI-2 deposited at 848°C according to thermocouples, or 863°C, allowing for a 15°C temperature drop between deposition surface and thermocouple. At 863°C, the saturated vapor pressure of antimony is 407 Pa;¹⁶ the partial pressure is

$$\frac{407 \text{ Pa}}{4.0 \times 10^{-3} \text{ Pa}} = 1.02 \times 10^5 \text{ less}.$$

Elemental antimony has a density of $6.684 \text{ g}\cdot\text{cm}^{-3}$, or

$$\frac{6.684}{121.75} \times 6.022169 \times 10^{23} = 3.31 \times 10^{22} \text{ atoms}\cdot\text{cm}^{-3} .$$

For deposition to occur, the platinum surface must have an antimony activity equivalent to

$$\frac{3.31 \times 10^{22}}{1.02 \times 10^5} = 3.25 \times 10^{17} \text{ atoms}\cdot\text{cm}^{-3} .$$

The flux of antimony deposits $2.7 \text{ }\mu\text{g}\cdot\text{cm}^{-2}$ in 20 min; the rate is

$$\frac{2.9 \times 10^{-6}}{121.75} \times \frac{6.022169 \times 10^{23}}{20 \times 60} = 1.2 \times 10^{13} \text{ atoms}\cdot\text{cm}^2\cdot\text{s}^{-1} .$$

Therefore,

$$D_{\min} = \frac{4 \times (1.2 \times 10^{13})^2 \times 20 \times 20}{\pi \times (3.25 \times 10^{17})^2} = 2.1 \times 10^{-6} \text{ cm}^2\cdot\text{s}^{-1} .$$

This value is very large, but can be reduced by making other assumptions. For instance, if antimony is released as a burst early in the test, it will be deposited at a higher partial pressure and diffusion need not be so rapid. Alternatively, if antimony reacts with platinum to reduce its own activity, a higher surface concentration can be tolerated before antimony reevaporates; for example, if antimony activity is reduced by 10, D_{\min} drops by 100.

APPENDIX E. DIFFUSION COEFFICIENT OF TELLURIUM IN PLATINUM

During a set of experiments on the isolation of tellurium adsorbed by platinum, some measurements were taken that enable the diffusion coefficient of tellurium in platinum to be calculated. In the experiments, platinum foil was exposed to tellurium traced with ^{129m}Te in steam at 900°C for 30 min. Two samples were then etched in aqua regia (75 vol % concentrated hydrochloric acid, 25 vol % concentrated nitric acid) for 30 min on a boiling water bath. The amounts of ^{129m}Te before and after were measured (all corrected for self-shielding):

	<u>Specimen 4</u> (μCi)	<u>Specimen 7</u> (μCi)
Pt before leaching	4.54 ± 0.05	3.17 ± 0.04
Pt after leaching	2.81 ± 0.01	1.93 ± 0.03
Leach solution	1.67 ± 0.03	1.18 ± 0.02
% recovery of ^{129m}Te	98.7 ± 1.4	98.1 ± 2.0
% ^{129m}Te removed	38.1 ± 0.9	39.1 ± 1.7

A 2.1-cm \times 2.2-cm sample of foil, of 100- μm nominal thickness, was etched with aqua regia under the same conditions, and the thickness was estimated by weighing, assuming platinum has a density of $21.45 \text{ g}\cdot\text{cm}^{-3}$.

<u>Duration of etch (min)</u>	<u>Weight (g)</u>	<u>Thickness (μm)</u>
0	0.9679	97.7
10	0.8976	90.6
27	0.8178	82.5

Based on these figures, the platinum would lose $16.9 \pm 0.8 \mu\text{m}$ in 30 min if the dissolution rate remains constant.

Both tellurium diffusion and acid dissolution occurred equally on both faces of the foil; of the tellurium that deposited on one face, $38.3 \pm 1.1\%$ was present in $8.7 \pm 0.4 \mu\text{m}$ of platinum after 1800 s at 900°C .

The tellurium deposited on the platinum surface at a varying rate during the 1800 s of the experiment, but for ease of numerical analysis we will consider the two extreme scenarios, in which the tellurium was either deposited all at once at the start of the time, or deposited at a constant rate throughout the period.

For the case where the tellurium was deposited all at once,

$$\frac{C}{C_0} = \text{erf} \left(\frac{x}{(4Dt)^{1/2}} \right)$$

where

C_0 = initial concentration, g/cm³,

C = final concentration, g/cm³,

$\frac{C}{C_0}$ = fraction of tellurium removed by acid = 0.383 ± 0.011 ,

x = depth of acid etch = $8.7 \pm 0.4 \times 10^{-4}$ cm,

t = duration of deposition experiment = 1800 s,

D = diffusion coefficient for Te in Pt in cm²·s⁻¹,

erf = the Gaussian error function: $\text{erf}(z) = \frac{2}{\pi^{1/2}} \int_0^z \exp(-t^2) \cdot dt$.

The diffusion coefficient by this treatment is $8.4 \pm 0.7 \times 10^{-10}$ cm²·s⁻¹.

For the case when the tellurium is deposited at a constant rate, the analysis is more complex. If M atoms·cm⁻² are deposited in an instant, we can utilize the following expression:²⁵

$$K = \frac{M}{(\pi D \tau)^{1/2}} \cdot \exp\left(\frac{-z^2}{4D\tau}\right),$$

where

z = position beneath platinum surface, cm

τ = time after atoms are deposited, s,

K = concentration of atoms at z and τ .

For a continuous source of F atoms·cm⁻²·s⁻¹,

$$K = \frac{F}{(\pi D)^{1/2}} \int_0^t \exp\left(\frac{-z^2}{4D(t-\tau)}\right) \cdot \frac{d\tau}{(t-\tau)^{1/2}}.$$

If acid etching removes the platinum down to x cm, the amount of tellurium removed is

$$C = \frac{F}{(\pi D)^{1/2}} \int_0^x \int_0^t \exp\left(\frac{-z^2}{4D(t-\tau)}\right) \cdot \frac{d\tau}{(t-\tau)^{1/2}} \cdot dz,$$

and the fraction removed becomes

$$\frac{C}{C_0} = \frac{1}{t} \int_0^t \text{erf}\left(\frac{x}{(4D\tau)^{1/2}}\right) \cdot d\tau,$$

where

$$\begin{aligned}\frac{C}{C_0} &= 0.383 \pm 0.011, \\ t &= 1800 \text{ s}, \\ x &= 8.7 \pm 0.4 \times 10^{-4} \text{ cm}.\end{aligned}$$

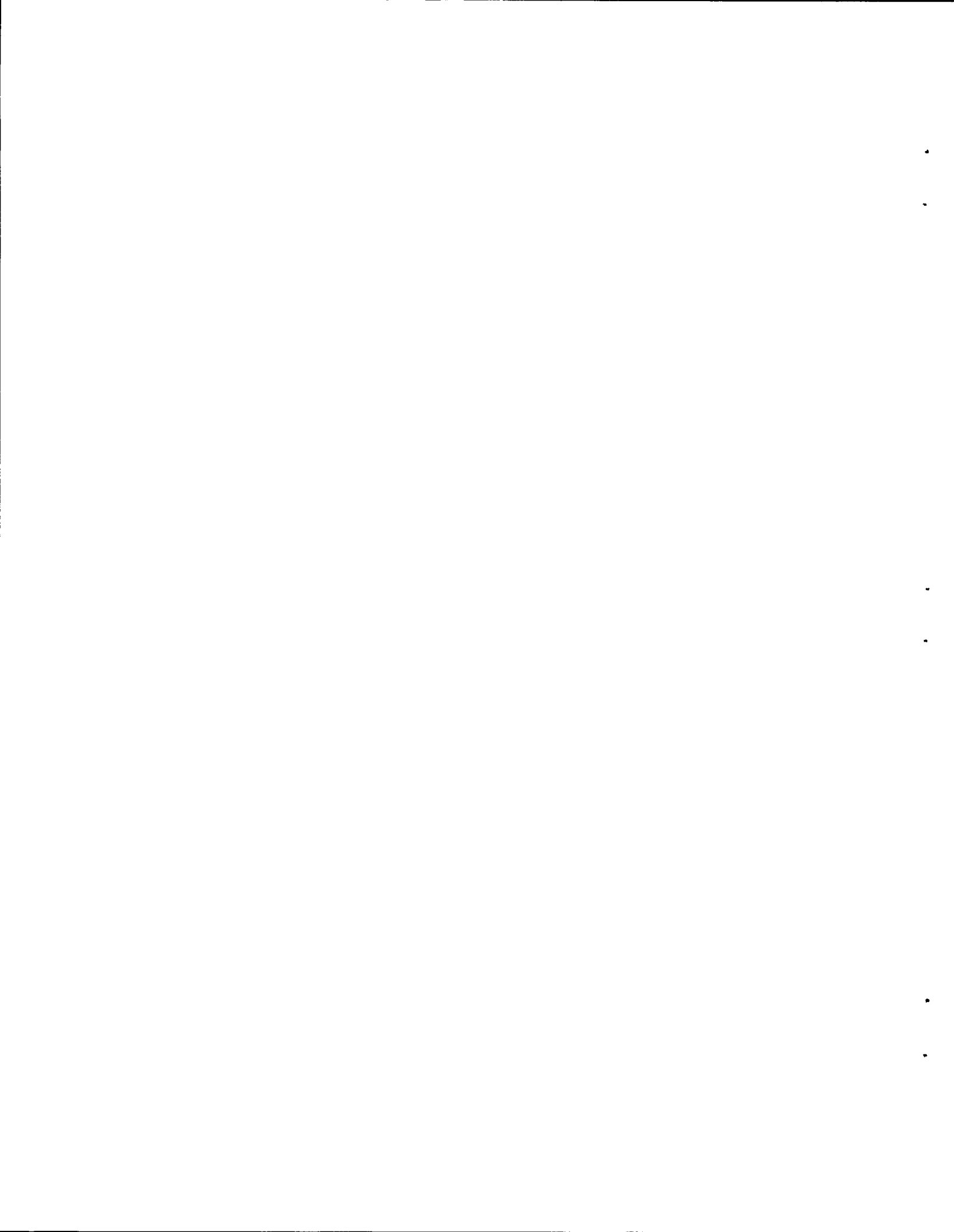
The diffusion coefficient by this treatment is $2.5 \pm 0.2 \times 10^{-9} \text{ cm}^2 \cdot \text{s}^{-1}$. To summarize, the diffusion coefficient of tellurium in platinum at 900°C lies in the range 8.4×10^{-10} to $2.5 \times 10^{-9} \text{ cm}^2 \cdot \text{s}^{-1}$, somewhat larger than the value of 6.5×10^{-14} to 9.0×10^{-14} for platinum in platinum and 6.1×10^{-13} for copper in platinum.²⁶ The Pt/Te system differs from the other two systems in that the compounds PtTe, Pt₃Te₄, and PtTe₂ are formed.²⁷ This may accelerate the diffusion process.

Solid state diffusion is an activated process, and the diffusion coefficient is temperature dependent:

$$D = D_0 \exp(-Q/RT) .$$

On average, $D_0 = 0.5 \text{ cm}^2 \cdot \text{s}^{-1}$, so approximate upper and lower bounds can be placed on $D(\text{Te in Pt})$ at all temperatures:²⁶

$$\begin{aligned}D_{\text{upper}} &= 0.5 \exp(-22400/T); & Q &= 186 \text{ kJ} \cdot \text{mol}^{-1} ; \\ D_{\text{lower}} &= 0.5 \exp(-23700/T); & Q &= 197 \text{ kJ} \cdot \text{mol}^{-1} .\end{aligned}$$



APPENDIX F. ESTIMATE OF THE ACTIVITY COEFFICIENT
OF ANTIMONY IN PLATINUM

The volatility of antimony above platinum/antimony alloys depends on its chemical potential, μ_{Sb} , where

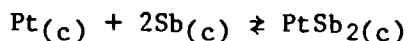
$$\mu_{\text{Sb}} = RT \ln a_{\text{Sb}} = RT \ln \gamma_{\text{Sb}} x_{\text{Sb}},$$

where

- $R = 8.31434 \text{ JK}^{-1}\cdot\text{mol}^{-1}$,
 $T = \text{temperature (K)}$,
 $a_{\text{Sb}} = \text{activity of antimony}$,
 $\gamma_{\text{Sb}} = \text{activity coefficient}$,
 $x_{\text{Sb}} = \text{mole fraction}$.

Because of compound formation, the volatility of one constituent of a binary alloy may be reduced: $\gamma < 1$. Typical values for γ_{Sb} are 0.505 in Ag/Sb and 0.26 in Cu/Sb.¹⁶ Platinum/antimony forms the compound PtSb_2 , which exists as the mole fraction of Sb decreases until it reaches 0.11; it then converts to a solid solution of Sb in Pt.²⁸ Throughout this range, the activity coefficient is < 1 , because PtSb_2 is stable.

The enthalpy of formation of PtSb_2 has not been measured, but for NiSb_2 it is $-76.6 \text{ kJ}\cdot\text{mol}^{-1}$. An estimate for the enthalpy of PtSb_2 might be:



$$\Delta H = -63 \text{ kJ}\cdot\text{mol}^{-1} \text{ PtSb}_2$$

$$\Delta S = 0.$$

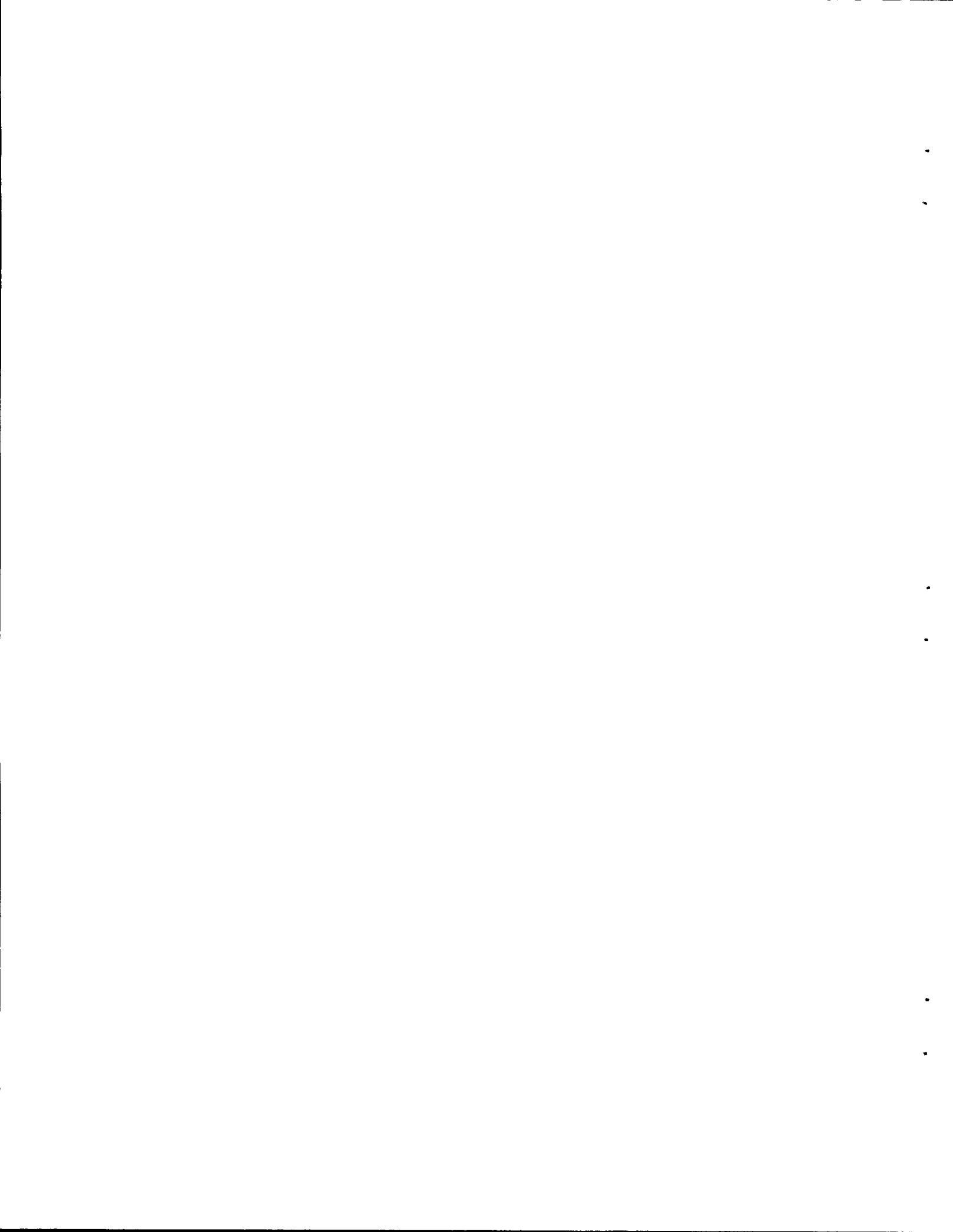
The chemical potential of Sb at equilibrium would be:

$$-31.5 \text{ kJ} = RT \ln a_{\text{Sb}}.$$

At 900°C , $a_{\text{Sb}} = 3.96 \times 10^{-2}$, when $x_{\text{Sb}} > 0.11$, since PtSb_2 is stable. When

$$x_{\text{Sb}} < 0.11, a_{\text{Sb}} = \gamma_{\text{Sb}} x_{\text{Sb}}, \text{ where } \gamma_{\text{Sb}} = 3.960 \times 10^{-2} / 0.11 = 0.36.$$

In conclusion, PtSb_2 formation depresses the saturated vapor pressure of Sb over Pt, by the amount of the activity coefficient, 0.36, at 900°C — and more at lower temperatures.



APPENDIX G. A METHOD FOR ANALYZING THE THERMAL GRADIENT TUBE FOR TELLURIUM

G.1 PREPARATION OF PLATINUM FOILS DEPOSITED WITH TELLURIUM

Figure G.1 illustrates the apparatus and the ampoules used. Eleven squares of platinum were cut, 2.0 cm on a side, from foil 100- μm thick. They were smoothed by rubbing with a PTFE rod, identified by scribing a number in each corner, and cleaned in boiling detergent solution for 30 min, followed by a wash in deionized water. Then they were loaded into the large silica vessel using long-handled tongs, and the hemispherical cap was sealed on.

One ampoule was loaded with sufficient water to provide a steam atmosphere of $<10^5$ Pa at 900°C. The linear dimensions of the main silica vessel indicated that its sealed volume would be >470 cm³; a 10^5 -Pa steam atmosphere at 900°C would contain 0.0880 g water. In fact, 0.0852 g was used. The ampoule and water were slowly immersed in liquid nitrogen to within 1 cm of the narrowed portion; this immobilized the water, but air could be removed by evacuation and backfilling with argon/4% hydrogen. The ampoule was sealed under vacuum.

The ORNL Isotopes Group prepared three evacuated ampoules containing ¹²⁸Te(element), activated by neutron bombardment to ^{129m}Te. One ampoule containing 36.8 ± 0.1 μCi ^{129m}Te in 4.5 mg ¹²⁸Te was set aside.

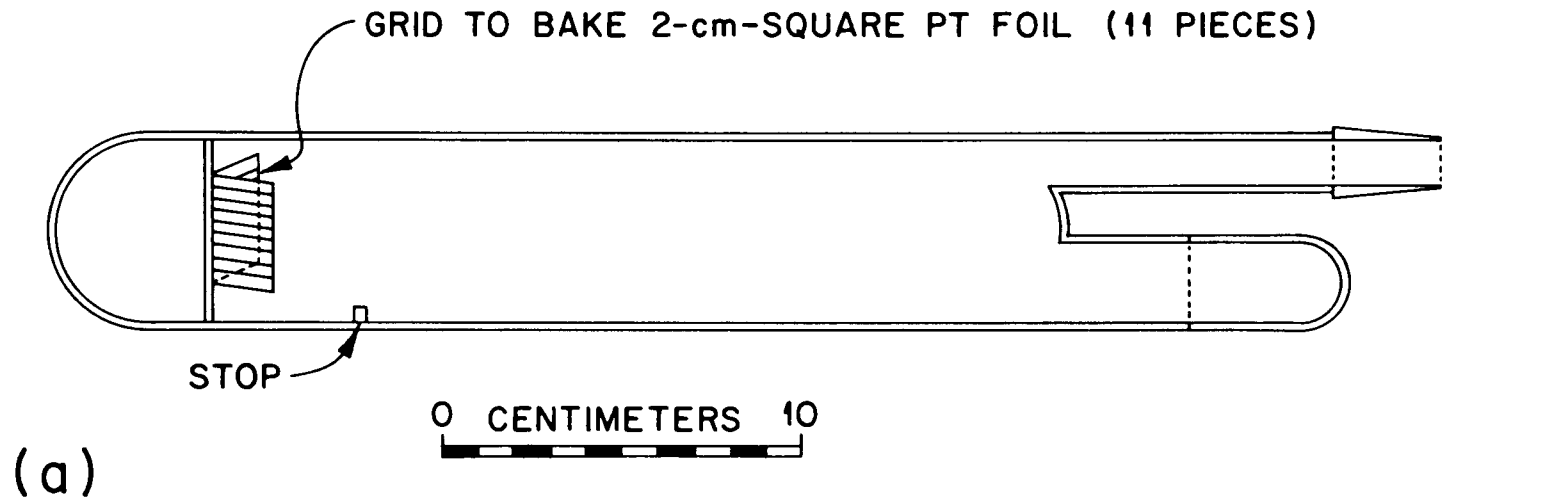
The other two ampoules were loaded, with magnetic breakers, into the silica vessel, which was flushed twice with argon/4% hydrogen and sealed under vacuum. The ampoules were broken magnetically and the vessel was heated to 900°C; Fig. G.2 illustrates a typical temperature history.

After the apparatus had cooled to room temperature, it was broken, and 11 platinum samples were removed and counted individually. The platinum samples had 1.8–4.5 μCi each of ^{129m}Te; in total, 34.9 ± 2.4 μCi was recovered on platinum, which compares well with the 36.8 ± 0.1 μCi initially present. The large error on the "after" measurement arose because it was difficult to measure the sample-to-gamma detector distance (8.0 ± 0.2 cm).

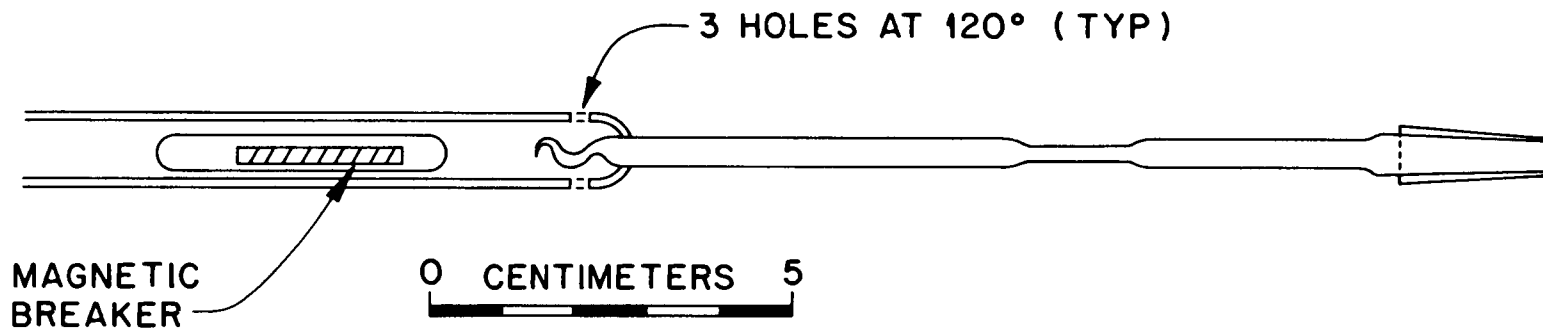
G.2 RESPONSE OF PLATINUM/TELLURIUM SAMPLES TO LEACHING

Five leaching tests were performed; the results are given in Table G.1. When prepared at 900°C, tellurium on platinum is inert to the basic ($\text{NH}_3/\text{H}_2\text{O}_2$) and acidic (HNO_3/HF) leaches used in the HI series of fission-product release tests. This implies that tellurium released in previous tests had been retained on the archived sections from the platinum thermal gradient tube, and these could be retrieved and analyzed.

Tellurium had diffused into the platinum to such an extent that the sample had to be completely dissolved to liberate it. Under the leaching conditions (footnote *g* in Table G.1), HCl/HNO_3 proved to be a suitable solvent.



(a)



(b)

Fig. G.1. Silica apparatus for preparing platinum foils deposited with tellurium.

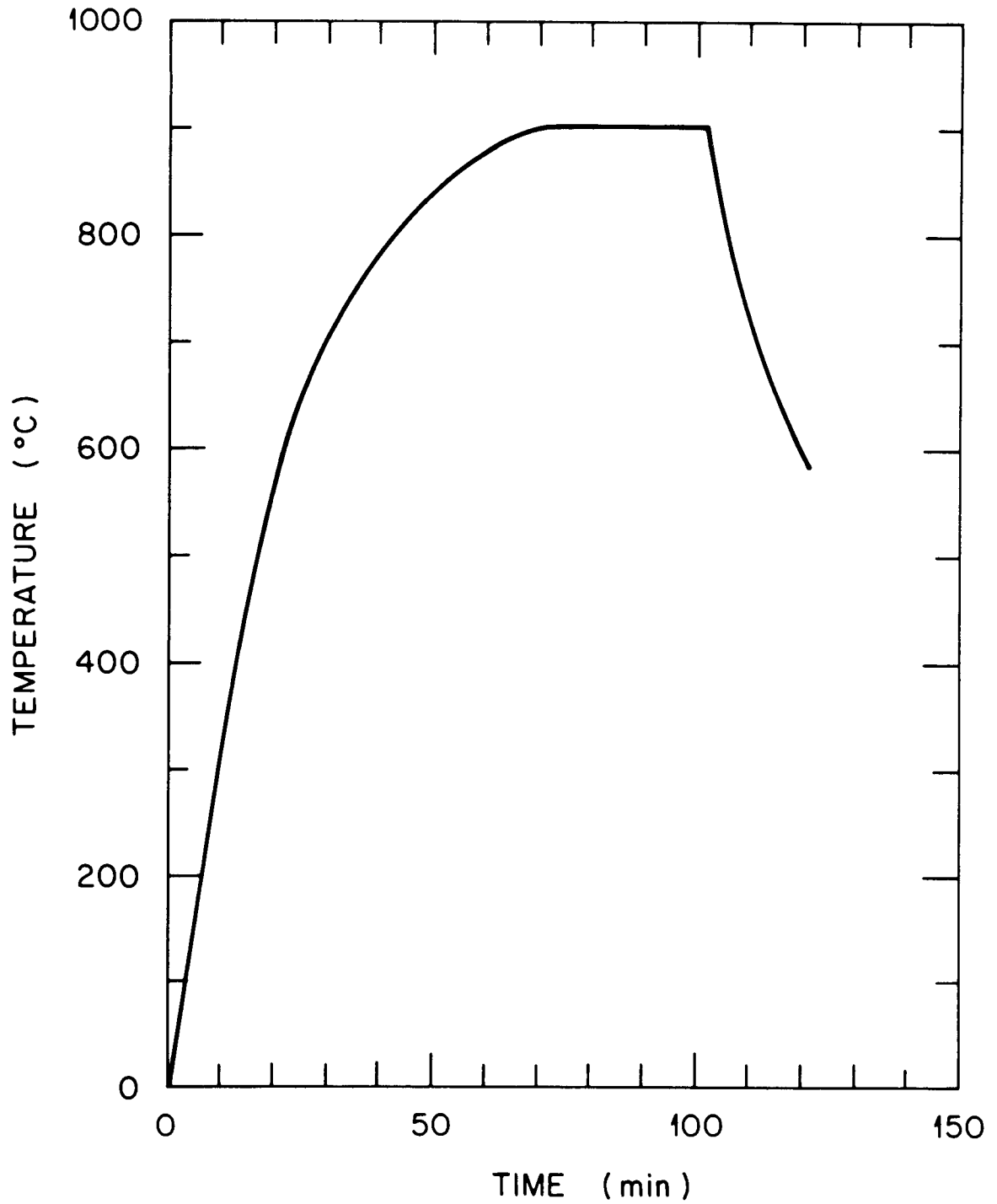


Fig. G.2. Temperature history of furnace during deposition of tellurium on platinum in steam.

Table G.1. Effects of leaches on tellurium deposited on platinum at 900°C

Leach type	^{129m}Te (μCi)			Pt leached (%)	Mass balance (%)
	On Pt before leach	On Pt after leach	In leach		
Water ^a	1.87 ± 0.03 ^b	NM ^e	<0.006	<0.3	
	3.60 ± 0.04	NM	<0.007	<0.2	
$\text{NH}_3/\text{H}_2\text{O}_2$ ^d	2.42 ± 0.03	NM	0.020 ± 0.007	0.8	
	3.79 ± 0.04	NM	0.011 ± 0.005	0.3	
HNO_3/HF ^e	2.28 ± 0.03	NM	0.018 ± 0.009	0.8	
	3.41 ± 0.04	NM	0.033 ± 0.010	1.0	
HCl/HNO_3 ^f	4.69 ± 0.05	2.90 ± 0.01	1.73 ± 0.03	37	99
	3.27 ± 0.04	1.99 ± 0.03	1.22 ± 0.02	37	98
HCl/HNO_3 ^g	1.87 ± 0.03	CD ^h	2.09 ± 0.03	112	
	3.60 ± 0.04	CD	3.70 ± 0.03	103	
	2.40 ± 0.03	NM	2.28 ± 0.02	95	
	3.78 ± 0.04	NM	3.33 ± 0.02	88	

^a 25 cm³ deionized water at 25°C for 2 h.

^b Gamma counting error. Real error may approach $\pm 7\%$, because it is difficult to measure the sample-detector distance.

^c NM = not measured.

^d 25 cm³ at 25°C for 2 h. Leach is 3 volumes concentrated NH_4OH and 1 volume 30% H_2O_2 .

^e 25 cm³ at 25°C for 2 h. Leach is 4 M HNO_3 , 0.25 M HF.

^f 10 cm³ at 100°C for 30 min. Leach is 3 volumes concentrated HCl and 1 volume concentrated HNO_3 .

^g 15 cm³ at 100°C for 1 h. Additional 10 cm³ at 100°C added for 1 more hour. Leach composition as for ^f.

^h CD = completely dissolved.

G.3 CONDITIONING OF SOLUTION BEFORE TELLURIUM PRECIPITATION

After acid dissolution, platinum and tellurium were present as chloro-complexes, probably PtCl_6^{2-} and TeCl_6^{2-} ; HNO_2 and NOCl may have been present.

The nitrogen compounds catalyzed the oxidation of SO_2 by HNO_3 , and so delayed tellurium precipitation. In a test where SO_2 was bubbled into an HCl/HNO_3 solution, brown nitrogen oxides evolved for an hour and no precipitate formed. When sulphamic acid was added to destroy HNO_2 and NOCl , no nitrogen oxides formed and precipitation began immediately.

Urea was chosen as the scavenger for HNO_2/NOCl because it was less likely than sulphamic acid to have Te contaminants.

Platinum co-precipitated with tellurium when SO_2 was used as a reductant; in the later stages of the analysis, it redissolved to PtCl_6^{2-} and overloaded the ion-exchange resin. Cyanide in basic solution converted the platinum to a stable tetracyanoplatinate(II), and prevented its precipitation:



Under some conditions, elemental selenium and tellurium also react with cyanide to form SeCN^- and TeCN^- , but the results of this study show such reactions do not affect the outcome of the tellurium analysis.

A three-fold excess of NaCN was used in the procedure.

Precipitation of tellurium on a carrier was necessary because it was present in only microgram quantities. Selenium is chemically similar and can be removed later by selective elution from the ion-exchange column.

Selenium was added as crystalline SeO_2 , which rapidly dissolved in hydrochloric acid solutions to form SeCl_6^{2-} .

G.4 PRECIPITATION OF TELLURIUM ON SELENIUM

Two precipitation methods²⁹ were tried: bubbling SO_2 through the solution, and the use of prepared solutions of SO_2 and $\text{N}_2\text{H}_6\text{Cl}_2$ in water.

The simplest method is to bubble SO_2 through. The precipitate settled readily but was difficult to filter, so this method was abandoned.

Reference 29 recommends SO_2 and $\text{N}_2\text{H}_6\text{Cl}_2$ for precipitation of tellurium. Tracer tests with $^{129\text{m}}\text{Te}$ gave the following results:

<u>μCi before pptn</u>	<u>μCi after pptn</u>	<u>% completeness</u>
2.28 ± 0.02	0.024 ± 0.16	99.0
2.62 ± 0.04	<0.03	98.9
3.33 ± 0.02	0.06 ± 0.02	98.2

The precipitate was granular and easy to filter.

G.5 PREPARATION OF ION-EXCHANGE RESIN LOADED WITH TELLURIUM

The precipitate was dissolved in HCl/HNO_3 , diluted, and treated with urea to remove nitrogen oxides that may degrade the ion-exchange resin. Care is needed in this step, because the precipitate may become colloidal and pass through undissolved. The final solution contains SeCl_6^{2-} and TeCl_6^{2-} in 3 M HCl .

The ion-exchange column was a modified polyethylene irradiation insert, exactly as described in Ref. 30.

The resin used was Dowex 1X-4 (50-100 mesh), a quarternary-ammonium type polystyrene available in the chloride form. The resin was stored in 3 M HCl and loaded into the columns as necessary.

Tellurium was adsorbed quantitatively as TeCl_6^{2-} from 3 M HCl ,³¹ but selenium was poorly adsorbed. A further elution with 5 column-volumes of 3 M HCl removed the remaining selenium. Typical tellurium losses would be:

	<u>μCi</u>
$^{129\text{m}}\text{Te}$ on platinum	2.62 ± 0.04
loss on precipitation	<0.03
loss on loading 1X column	0.15 ± 0.02
loss on eluting selenium	0.12 ± 0.02

Transfer of tellurium from platinum to the ion-exchange column is >88% complete in this case.

One blank was neutron activated, and $0.1 \text{ nCi } ^{75}\text{Se}$ was detected on the ion-exchange resin. This represents a decontamination factor of 9×10^4 for selenium.

No platinum activation products were observed.

G.6 APPLICATION

No tellurium-containing, ion-exchange resins have been activated, because one blank resin bed was incompletely dried and split under irradiation. Attempts have been made to elute the tellurium in 0.15 M HCl and evaporate to dryness. The residue has then been neutron activated, but no tellurium could be detected.

Tellurium samples from the HI series of fission product release tests are ~70% ^{130}Te , which is activated to 30-h ^{131}Te , decaying to 8-d ^{131}I . The gamma spectrometer used in the release tests could detect 5×10^{-3} counts/second at the 364.5 keV gamma of ^{131}I , so the technique has a theoretical sensitivity of ~30 ng tellurium.

G.7 APPLICATION TO A STAINLESS STEEL THERMAL GRADIENT TUBE

Observations indicate that tellurium dissolves fairly readily in the basic leach ($\text{NH}_3/\text{H}_2\text{O}_2$); the solution may be made 3 M in HCl and the desorbed isolation procedure carried out (Sect. 7). The hydrogen peroxide may need to be destroyed catalytically with MnO_2 before adding SO_2 and $\text{N}_2\text{H}_6\text{Cl}_2$.

Stainless steel dissolves in acid to form products that do not coprecipitate with selenium and tellurium, so no masking with cyanide is required.

G.8 PROCEDURE

1. Digest platinum foil sample (<1.0 g) with 15 mL aqua regia (3 parts concentrated hydrochloric acid and 1 part concentrated nitric acid) for 1 h on a boiling water bath.
2. Add a further 10 mL aqua regia and heat for another hour. The platinum will be almost completely dissolved, and the solution should be golden-yellow.
3. Add 1 g urea and 25 mL water and allow to stand for 15 min.
4. Add 3 drops m-cresolsulphonephthalein as pH indicator and use sodium hydroxide solution (11 g in 50 mL water) to make slightly alkaline. About 30 mL alkali is needed.
5. Carefully add 5 g sodium cyanide in 10 mL water and heat on a boiling water bath for 30 min. The solution fades to a straw color.
6. Allow to cool for 15 min and carefully add 40 mL of concentrated hydrochloric acid (solution should be about 3 M in hydrogen ion).
7. Add 28 ± 1 mg selenium dioxide and swirl to dissolve.
8. Bring to a boil on a hot plate and add in sequence:
 - 15 mL water freshly saturated with sulphur dioxide;
 - 10 mL of 15 g hydrazinium dichloride ($\text{N}_2\text{H}_6\text{Cl}_2$) made up to 100 mL with water and filtered; and
 - 25 mL water freshly saturated with sulphur dioxide.

Bring to a boil again and boil for 5 min; then allow to cool. A brick-red to black, granular precipitate of selenium and tellurium settles.

9. Filter through a medium glass frit, assisted by suction. Rinse precipitates with 10 mL 3 M hydrochloric acid.
10. Dissolve precipitate on filter with 2.0 mL aqua regia, added in small quantities. Wash through with 3.5 mL 0.2 M hydrochloric acid.
11. Add 0.1 g urea and warm on a boiling water bath for 5 min; then allow to cool.
12. Pass through a column of Dowex 1X-4 ion-exchange resin (50-100 mesh) preconditioned in 3 M hydrochloric acid, at 1 drop per second.
13. Pass 3.5 mL (5 column volumes) 3 M hydrochloric acid at 1 drop per second to elute selenium.
14. Dry column thoroughly by passing warm air through, and determine tellurium by neutron activation analysis.

G.9 ACKNOWLEDGMENTS

The author gratefully acknowledges the help of L. C. Bate (deceased) in irradiating samples in HFIR and R. Poole and the glassblowers for making the apparatus and helping to seal it.

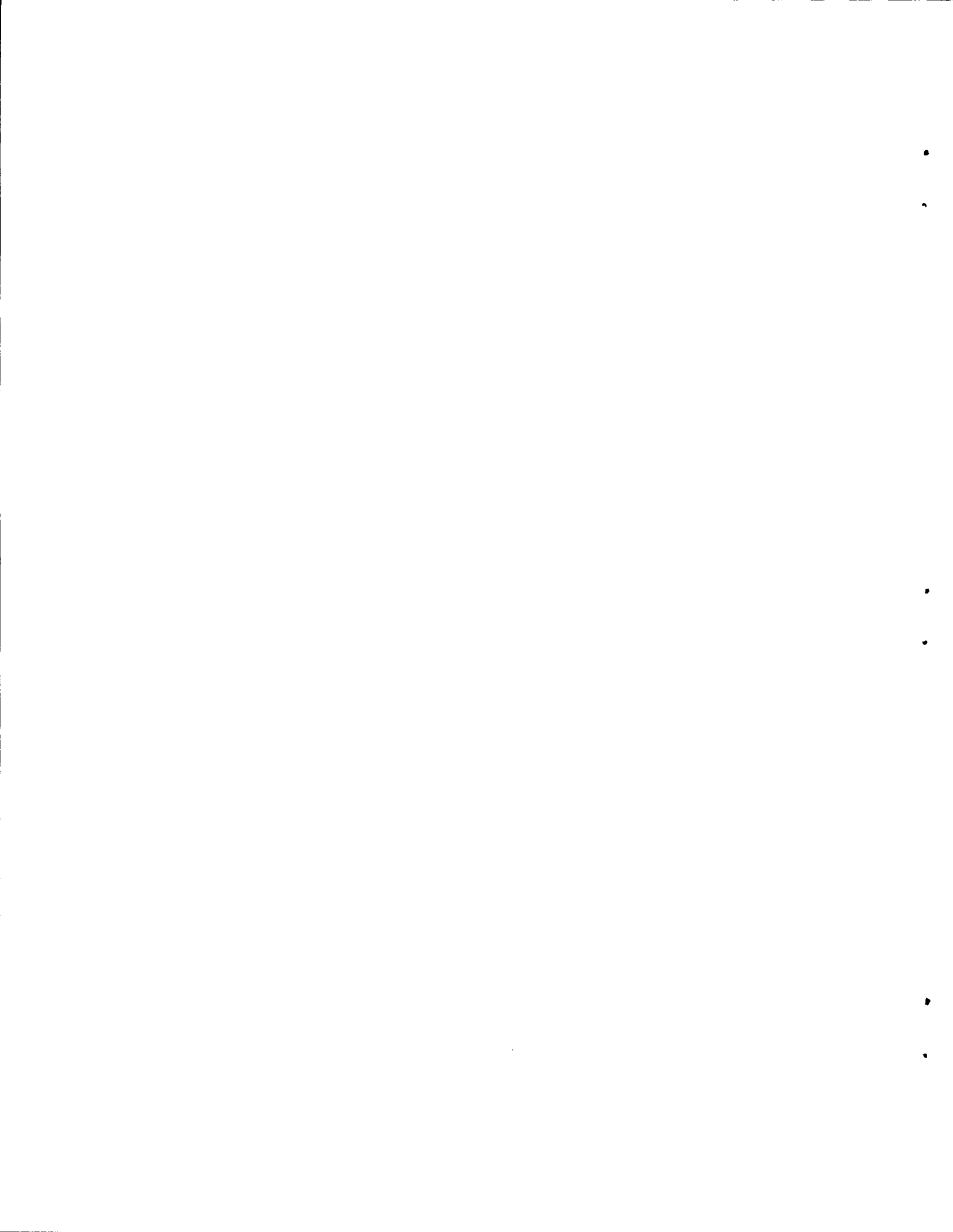
NUREG/CR-4105
 ORNL/TM-9506
 Dist. Category R3

INTERNAL DISTRIBUTION

- | | |
|-----------------------|---------------------------------|
| 1. R. E. Adams | 22. R. D. Spence |
| 2. C. W. Alexander | 23. M. G. Stewart |
| 3. E. C. Beahm | 24. O. K. Tallent |
| 4. L. H. Bell | 25. L. M. Toth |
| 5. J. T. Bell | 26. R. L. Towns |
| 6. J. L. Collins | 27. J. R. Travis |
| 7. R. W. Glass | 28. C. S. Webster |
| 8. J. R. Hightower | 29. S. K. Whatley |
| 9. E. K. Johnson | 30. R. P. Wichner |
| 10. T. S. Kress | 31. A. L. Wright |
| 11. C. E. Lamb | 32. R. G. Wymer |
| 12. T. B. Lindemer | 33. Central Research Library |
| 13. R. A. Lorenz | 34. ORNL-Y-12 Technical Library |
| 14. A. P. Malinauskas | Document Reference Section |
| 15. F. R. Mynatt | 35-36. Laboratory Records |
| 16-20. M. F. Osborne | 37. Laboratory Records, ORNL-RC |
| 21. G. W. Parker | 38. ORNL Patent Section |

EXTERNAL DISTRIBUTION

39. Office of Assistant Manager for Energy Research and Development, ORO-DOE, P.O. Box E, Oak Ridge, TN 37831
- 40-41. Director, Division of Reactor Safety Research, U.S. Nuclear Regulatory Commission, Washington, DC 20555
- 42-43. Technical Information Center, DOE, Oak Ridge, TN 37831
44. Division of Technical Information and Document Control, U.S. Nuclear Regulatory Commission, Washington, DC 20555
45. L. K. Chan, Fuel Systems Research Branch, Division of Accident Evaluation, U.S. Nuclear Regulatory Commission, Washington, DC 20555
- 46-50. K. S. Norwood, Chemical Technology Division, B10.5, AERE Harwell, Didcot, Oxon OX11 0RA, England
- 51-325. Given distribution as shown in Category R3 (NTIS - 10)



NRC FORM 335 (2-84) NRCM 1102, 3201, 3202		U.S. NUCLEAR REGULATORY COMMISSION		1 REPORT NUMBER (Assigned by TIDC add Vol. No., if any)	
2 TITLE AND SUBTITLE An Assessment of Thermal Gradient Tube Results from the HI Series of Fission Product Release Tests		3 LEAVE BLANK		4 DATE REPORT COMPLETED	
				MONTH March	YEAR 1984
5 AUTHOR(S) K. S. Norwood Guest scientist from UKAEA - Harwell		8 PROJECT TASK WORK UNIT NUMBER		5 DATE REPORT ISSUED	
				MONTH March	YEAR 1985
7 PERFORMING ORGANIZATION NAME AND MAILING ADDRESS (Include Zip Code) Oak Ridge National Laboratory P.O. Box X Oak Ridge, TN 37831		9 FIN OR GRANT NUMBER B0127		11a TYPE OF REPORT NUREG	
				b PERIOD COVERED (Inclusive dates)	
10 SPONSORING ORGANIZATION NAME AND MAILING ADDRESS (Include Zip Code) U.S. Nuclear Regulatory Commission Division of Accident Evaluation Fuel Systems Research Branch Washington, DC 20555		12 SUPPLEMENTARY NOTES			
13 ABSTRACT (200 words or less) A thermal gradient tube was used to analyze fission product vapors released from fuel heated in the HI test series. Complete deposition profiles were obtained for Cs, I, Ag, and Sb. The cesium profiles were complex and probably were dominated by Cs-S-O compounds formed by release of sulfur from furnace ceramics. The iodine profiles were simple, indicating that more than 99.5% of the released iodine behaved as a single nonvolatile species, probably CsI. Mass transfer coefficients for this species onto platinum were estimated to be 1.9 to 5.8 cm/s. Silver was probably released in elemental form, condensed to an aerosol, and captured by filters. Antimony was released as the element and reacted rapidly with platinum (or gold) as it deposited. Antimony profiles were calculated <u>a priori</u> with some success. A method was developed for isolating tellurium from platinum and mixed fission products in a form suitable for neutron activation analysis. The platinum samples were completely dissolved in acid (HCl/HNO ₃), and the tellurium was precipitated on selenium carrier by reduction. Finally, tellurium was loaded onto Dowex 1X-4 ion-exchange resin for activation and analysis. Tellurium recovery was ~88%, and the theoretical sensitivity was ~30 ng.					
14 DOCUMENT ANALYSIS -- KEYWORDS/DESCRIPTORS Fission product Fission product chemistry Thermal gradient tube b IDENTIFIERS OPEN ENDED TERMS				15 AVAILABILITY STATEMENT	
				16 SECURITY CLASSIFICATION <i>(This page)</i> Unclassified <i>(This report)</i> Unclassified	
				17 NUMBER OF PAGES 59	
				18 PRICE	